

# DISSERTATION

Titel der Dissertation

**Nanoparticles of biodegradable polymers and  
DPPC liposomes for skin diffusion studies and  
physicochemical stabilisation of the  
incorporated model drugs**

Verfasserin

Mag. Amra Hasanovic

angestrebter akademischer Grad

Doktorin der Naturwissenschaften (Dr. rer. nat.)

Wien, 2010

Studienkennzahl lt Studienblatt:

A 449

Dissertationsgebiet lt. Studienblatt:

Pharmazie

Betreuerin / Betreuer:

ao. Univ.-Prof. Dr. Claudia Valenta



## **Danksagung**

Mein besonderer Dank gilt Frau a.o.Univ.-Prof Dr. Claudia Valenta für ihre Betreuung und ihre große Unterstützung in zahlreichen Diskussionen sowie für die familiäre und freundschaftliche Atmosphäre in der Arbeitsgruppe.

Weiters bedanke ich mich bei allen meinen Kollegen und Diplomanden für ihre Unterstützung und Hilfsbereitschaft besonders bei Arvid Staub für das Liposom-Bild.

Außerdem danke ich a.o.Univ.-Prof Dr. Gottfried Reznicek and Dr. Martin Zehl für die Zusammenarbeit sowie Dr. Günter Resch für die Kryo-TEM Aufnahmen und interessanten fachlichen Diskussionen.

Ich bedanke mich auch beim Prof. Dr. Dr. Jürgen Lademann, Charité, und seiner Arbeitsgruppe für die Einschulung in die „Tape stripping“ Studien.

Ganz besonderer Dank gilt meinen Eltern, die mich immer unterstützt und gefördert haben.

## Table of content

<b>1</b>	<b>Einleitung und Zielsetzung.....</b>	<b>1</b>
<b>2</b>	<b>Introduction and Aim of the study.....</b>	<b>3</b>
<b>3</b>	<b>Background .....</b>	<b>5</b>
3.1	Skin .....	5
3.1.1	Structure and morphology of the skin .....	5
3.1.2	Mechanisms of skin penetration .....	10
3.2	Mechanisms of enhancement .....	12
3.3	Nanoparticles .....	14
3.3.1	Polymeric nanoparticles.....	14
3.4	Lipid based particles .....	18
3.4.1	Liposomes .....	18
<b>4</b>	<b>Specific topics .....</b>	<b>22</b>
4.1	Chitosan-TPP nanoparticles as a possible skin drug delivery system for aciclovir with enhanced stability.....	22
4.2	Improvement of physicochemical parameters of DPPC liposomes and increase of skin permeation of aciclovir and minoxidil by addition of cationic polymers.....	41
4.3	Modification of the conformational skin structure by treatment with liposomal formulation and its correlation to the penetration depth of aciclovir .....	62
4.4	Analysis of skin penetration of phytosphingosine by fluorescence detection and influence of the thermotropic behaviour of DPPC liposomes.....	79
<b>5</b>	<b>Conclusion.....</b>	<b>92</b>
<b>6</b>	<b>References.....</b>	<b>94</b>
<b>7</b>	<b>List of scientific publications, within the present work.....</b>	<b>100</b>
7.1	Publications .....	100
7.2	Poster presentations.....	100
7.3	Oral presentations .....	100
<b>8</b>	<b>List of Scientific publications, beyond the present work .....</b>	<b>101</b>
8.1	Publications .....	101
8.2	Poster presentations.....	101
<b>9</b>	<b>Abbreviations .....</b>	<b>102</b>



## 1 Einleitung und Zielsetzung

Die dermale Applikation kann zur Behandlung oberflächlicher oder systemischer Hautdefekte angewendet werden. Diese Möglichkeit bietet gegenüber den klassischen Applikationswegen enorme Vorteile, wie die Umgehung des First-Pass Effektes bei oraler Verabreichung oder die negativen Auswirkungen invasiver parenteraler Applikationsformen. Um die systemische Wirkung zu erzielen muss zuerst die Hauptpenetrationsbarriere, das Stratum corneum, überwunden werden. In diesem Fall kann durch Zusatz von Penetrationsförderern die Wirkstoffaufnahme verbessert werden. Solche verwendete Beschleuniger sind zum Beispiel Tenside bzw. Co-Tenside, aber auch die Auswahl der Vehikel spielt eine wichtige Rolle.

In den letzten Jahren sind Nanopartikel im medizinisch-pharmazeutischen Bereich intensiv untersucht worden, jedoch nicht im Hinblick auf die dermale Applikation [1]. Daher sollte im ersten Teil der vorliegenden Arbeit geprüft werden, ob bestimmte polymere Nanopartikel eventuell einen positiven Einfluss auf die Hautpermeation ausüben könnten. Aus diesem Grund sind polymere Nanopartikel bestehend aus Chitosan (CS) und Tripolyphosphat (TPP) auf der Haut getestet worden. Das erste Ziel war stabile und homogene CS-TPP Nanopartikel herzustellen und mit dem Modellarzneistoff Aciclovir zu beladen, weiters sollte neben der Erhöhung der chemischen Stabilität eine Diffusionsverbesserung des Modellarzneistoffes Aciclovir erreicht werden. Der zweite Teil beschäftigt sich mit DPPC Liposomen, mit ihrer Herstellung und ihrer physikochemischen Stabilisierung durch Umhüllung mit zwei kationischen Polymeren, Chitosan (CS) und Eudragit EPO (EU). Dabei war es das Ziel durch die kationischen Gruppen das Zetapotential so stark zu erhöhen, dass keine Zerstörung des kolloidalen Systems mehr möglich sein würde. Weiterhin sollten diese beiden Polymere durch ihre positive Ladung als Penetrationsförderer für die Hautdiffusion der beiden Modellarzneistoffe Aciclovir und Minoxidil dienen. Die Diffusionsstudien von Aciclovir sind neben der Franz-Zelle zusätzlich mittels „Tape Stripping“ durchgeführt worden. Die möglichen auftretenden Wechselwirkungen der DPPC Liposomen mit Chitosan und Eudragit EPO,

sowie auch zusätzlich mit den Arzneistoffen Minoxidil und Aciclovir sollten noch mittels der biophysikalischen Methoden ATR-FTIR und microDSC analysiert werden. Zusätzlich sollte die FTIR Spektroskopie zur Charakterisierung der humanen und porcinen Haut herangezogen werden. Eine Konformationsänderung der charakteristischen Lipid Schwingungen nach Einwirkung polymer-haltigen und polymer-freien liposomaler Formulierungen sollte belegt werden. Darüber hinaus stellte sich die Frage, ob diese Resultaten mit jenen der Aciclovir-Hautpenetration ermittelt durch „Tape Stripping“ korreliert werden können.

In vorangegangenen Studien konnte gezeigt werden, dass das in der Haut vorkommende Phytosphingosin (PS) imstande war die Hautpermeation von Fludrocortisonacetat und Flumethasonpivalat zu steigern [2]. Da der Wirkungsmechanismus nicht geklärt war, sollten zur Aufklärung weiterführende Untersuchungen getätigt werden. Zu diesem Zweck sollten im dritten Teil dieser Arbeit erneut Hautdiffusionsstudien, mit dem Ziel durchgeführt werden, zu analysieren wie viel PS in der Haut gespeichert bleibt. Dazu wurden DPPC Liposomen als Träger eingesetzt. Voraussetzung war eine geeignete sehr sensitive Analytik für PS. Es wurde eine Derivatisierung mit o-Phthalaldehyd (OPA-Reagens) und anschließender Fluoreszenzdetektion verwendet. Darüber hinaus sollten noch mögliche erwartete Wechselwirkungen von PS mit Modell-Lipiden in DSC-Untersuchungen herausgefunden werden.

## 2 Introduction and Aim of the study

Dermal applications can be used to treat either superficial or systemic skin defects. Such procedures can have tremendous advantages over conventional applications, such as avoidance of the first-pass effect and of adverse impacts arising from invasive parenteral application forms. To achieve the desired effects the main penetration barrier, the stratum corneum, has first to be overcome. Penetration can be improved by the addition of penetration enhancers. The most commonly used enhancers are surfactants or co-surfactants, but the range of vehicles can also play an important role.

In recent years, nanoparticles have been extensively studied in medical as well as in pharmaceutical fields, but little is known about their potential to penetrate the skin [1]. The first part of this thesis therefore investigated whether polymeric nanoparticles can have a positive influence on skin penetration. The effect of polymeric nanoparticles consisting of chitosan (CS) and tripolyphosphate (TPP) on skin was examined. The first goal was to produce stable and uniform CS-TPP nanoparticles that could improve penetration and chemical stability of the model drug aciclovir.

The second part of this work deals with DPPC liposomes. Their preparation and physicochemical stabilization by coating with two cationic polymers, either chitosan (CS) or eudragit EPO (EU), was analysed. Due to their positive charge these polymers should enhance the penetration of two model drugs, aciclovir and minoxidil. Interactions of DPPC liposomes with the polymers as well as with the model drugs were analyzed by FTIR and microDSC. In vitro diffusion studies with porcine skin using the Franz-cell model as well as the “tape stripping” method were performed to ascertain the penetration profile of aciclovir from different liposomal formulations. Moreover, FTIR spectroscopy was used to characterise human and different types of porcine skin. Finally, in order to find supporting evidence for the tape stripping studies, after skin treatment with polymer containing and polymer free liposomal formulations conformational changes of skin lipids were analysed by FTIR.



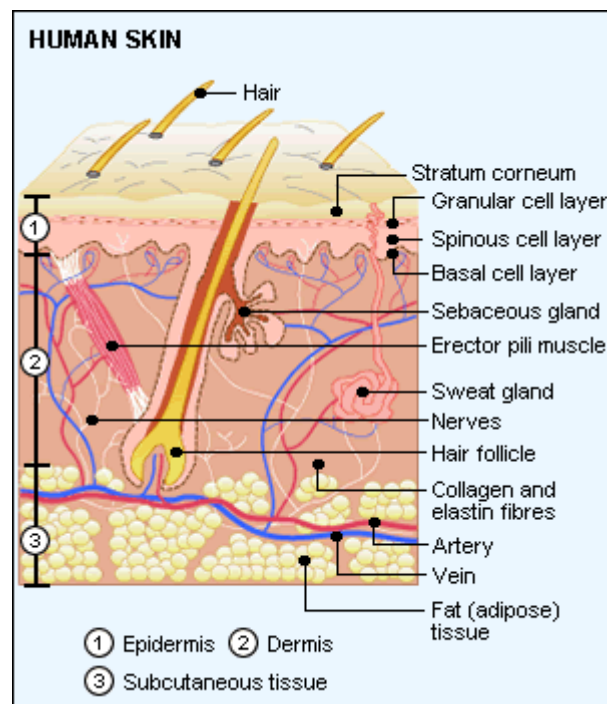
Previous studies have shown that phytosphingosine (PS), an active substance occurring in the epidermis, improved skin penetration of fludrocortisonacetate and flumethasonpivalate [2]. Therefore, in the third part of this thesis skin diffusion studies of PS were performed to demonstrate its penetration profile. The DPPC liposomes were used as a carrier for PS. In addition, a suitably sensitive technique was needed to determine PS content: to increase PS analytical sensitivity, PS was derivatised by o-phthalaldehyde (OPA) reagent and analysed by HPLC with fluorescence detection. Furthermore, possible interactions between the model-lipids and the sphingoid drug were investigated by microDSC.

### 3 Background

#### 3.1 Skin

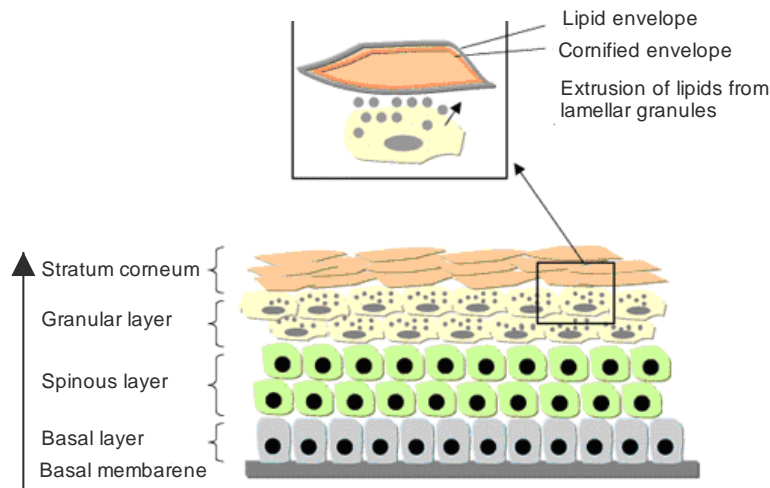
##### 3.1.1 Structure and morphology of the skin

Skin is our largest organ. It is made up of multiple layers of epithelial tissues, and guards the underlying muscles, bones, ligaments and internal organs. Due to its interfaces with the environment, skin plays a very important role in protecting the body from different dangers such as chemicals, bacteria, allergens, fungi and radiation. Skin also provides a barrier function that keeps moisture in, minimizing transepidermal water loss (TEWL). As figure 1 shows skin consists of four layers, stratum corneum (nonviable epidermis, 10-20  $\mu\text{m}$  thick), the viable epidermis (50-100  $\mu\text{m}$  thick), dermis and subcutaneous tissue as well as of the appendages like hair follicle, sebaceous, sweat glands [3, 4].



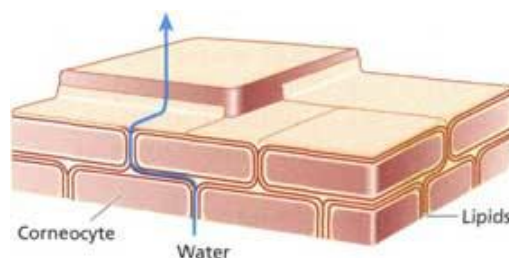
**Figure 1** Skin layers: epidermis, dermis and subcutaneous tissue, showing a hair follicle, sweat gland, sebaceous gland and other skin appendages (<http://www.treatment-skincare.com/Glossary/Skin-Structure-Diagram.html> access date: July 10)

Figure 2 represents stratum corneum (nonviable epidermis) and the layers of viable epidermis, stratum granulosum, stratum spinosum and stratum basale.



**Figure 2** Epidermis: stratum corneum, stratum granulosum, stratum spinosum and stratum basale ([http://www.medscape.com/viewarticle/564078\\_2](http://www.medscape.com/viewarticle/564078_2), access date: August 10)

On the basement membrane there is single layer of cuboidal basal keratinocytes that divide approximately every 28 days. After division, half of the keratinocytes undergo differentiation and become wider and flatter as they move towards the outermost skin layer, the stratum corneum. Finally, in the stratum corneum the end product of keratinisation process is an array of very flat, keratin-filled cells, bounded by cornified envelopes and embedded in a lipid matrix (Figure 2) [5]. The outermost layer of the skin, the stratum corneum, is only 10–20  $\mu\text{m}$  thick across most parts of the human body, but provides a formidable barrier to the passive permeation of drugs [6]. The stratum corneum has been also schematically represented as an idealised two-compartment model, “bricks and mortar” model, where the corneocytes representing the bricks and the lipid lamellae being the mortar (Figure 3) [7]. It has been proposed that these intercellular lipids play a fundamental role in the function and maintenance of the skin barrier [8].



**Figure 3** The multi-layered brick and mortar model of the stratum corneum (<http://www.pgbeautygroomingscience.com/the-epidermis.html>, access date: August 10)

The physical properties of the lipid mixture of the stratum corneum provide for greater permeation resistance than is found with more typical membrane lipids, such as phospholipids and cholesterol. According “to the domain mosaic model of the skin barrier” suggested by FORSLIND, lipids are organised in ordered domains (orthorhombic (OR) and hexagonal (HEX)) connected by lipids in a disordered (liquid-crystalline (LIQ)) phase (Figure 4) [9, 10].

Furthermore, more than one-third of human stratum corneum lipids have chain lengths longer than 22 carbons. Compared to the chain lengths of 16-18 carbons found in the cell membranes of living mammalian cells, this is quite remarkable and most certainly has functional implications [10].

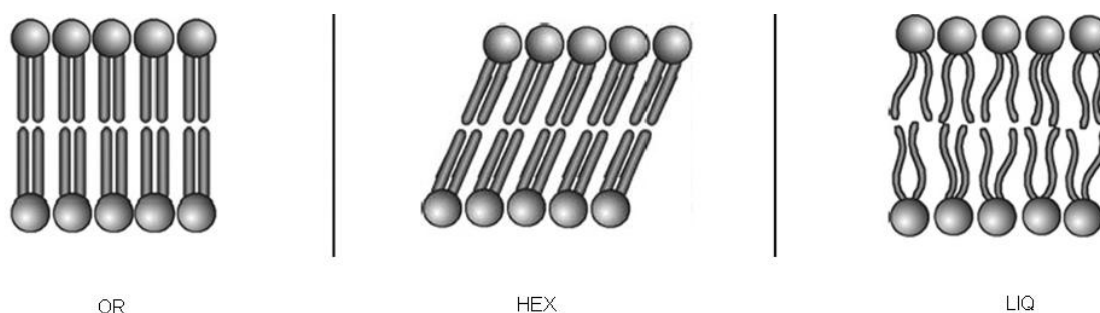


**Figure 4** Molecular organizations of stratum corneum lipids. Scheme of the chain conformation in orthorhombic (OR), hexagonal (HEX), and liquid-crystalline (LIQ) phases of long-chain lipids [9]

The intercellular lipids of stratum corneum consist of several different types of polar lipids dominated by ceramides (ca. 50 %), cholesterol (ca. 25 %) as well as free fatty acids (ca. 10 %) and small amounts of cholesterol sulphate

(2-5 %), which plays an important role in the desquamation process of stratum corneum [4, 5, 10]. Unlike all other biological membranes, those in the stratum corneum do not contain phospholipids [5, 11].

Ceramides provide a major component of the barrier function of the stratum corneum. The ceramides are structurally heterogeneous. Humans have 9 series of ceramides. The base component can be sphingosine, phytosphingosine or 6-hydroxysphingosine [12]. The most crucial of all the ceramides in the stratum corneum is the ceramid 1 consisting of phytosphingosine base with an amid-linked  $\omega$ -hydroxy fatty acid esterified to the  $\omega$ -hydroxyl group [13]. The other ceramides contain normal or  $\alpha$ -hydroxy acids amide-linked to one of the bases [12]. Due to its unique structure, ceramid 1, an acylceramide, may function as a stabiliser of the intercellular lipid lamellae. It is possible that ceramid 1 performing as a “molecular rivet” in the intercellular lipid lamellae of the stratum corneum [3, 13].

The last ten years have brought interesting observations about the barrier function of tight intercellular adhesion between keratinocytes. So called “tight junctions” (TJ) play a central role in sealing the intercellular space of cell sheets. Within the TJ, aqueous pores or paracellular channels are postulated to exist, which allow the controlled diffusion of water and solutes via the paracellular pathway [14, 15]. TJ are very complex structures, which consist of more than 40 proteins including transmembrane as well as of plaque proteins and have been demonstrated only in the stratum granulosum whereas tight junctions proteins (claudin 1 and 7) are found in all viable layers as well as in skin appendages and dermal blood vessels [14-17]. The TJ and its adhesion molecules have not been thought for crucial in the barrier function of the epidermis. However, their importance has been demonstrated in skin with impaired function (psoriasis or atopic dermatitis) [15, 17]. In addition, it seems likely now that modulation of TJ and its structures might lead to changes in skin permeability suggesting TJ for good target in skin delivery [17-20].

Moreover, the epidermis consists of melanocytes, sensory Merkel-cells, immunological active Langerhans-cells and lymphocytes beside two major keratinic cell types, the first having the capacity to divide and produce new

cells, the second serving to anchor the epidermis to the basement membrane [3].

The next skin layer, the dermis, is tightly connected to the epidermis by a basement membrane and provides the nutritive, immune and other support systems for the epidermis through the thin papillary layer. The dermis is about 0.1-0.5 cm thick and consists of collagenous fibres, providing flexibility via scaffold of support and elastic connective tissue. The lower reticular layer contains the main components of dermis such as blood vessels, lymph vessels, hair follicles, and glands that produce sweat (which helps regulate body temperature) and sebum, an oily substance protecting skin from drying out [3, 21]. The subcutaneous tissue or hypodermis is directly underlying the dermis and is mainly composed of adipose tissue. This layer is important in the regulation of skin and body temperature. The size of this layer varies throughout the body and from person to person. Its physiological function includes insulation and storage of nutrients and mechanical protection [21].

Ideally, human skin should be used to evaluate the penetration properties of model drugs. However, ethical problems, religious restrictions and limited availability make the use of human skin difficult for most researchers. Numerous animal models have been used as a substitute for human skin as pig, mouse, guinea pig, rat and snake skin. Most of the permeation studies conducted in pigs have been performed on their back, on the ear and few on the flank or abdomen. Various anatomical and physiological investigations show comparable characteristics between human skin and porcine ear skin in relation to the stratum corneum, epidermal thickness as well as follicular structure and hair density [22]. According to published data, the flux through the skin and concentration in the skin were of the same order of magnitude as in pig as in human skin, with differences of at most two- or fourfold, respectively [23-25]. Recently published results of analyses of the follicular penetration report about porcine ear skin being a more suitable in vitro model than excised human skin [26].

### 3.1.2 Mechanisms of skin penetration

The stratum corneum is known to be a major hindrance to the penetration of compounds into the skin. Additionally, molecules applied to the skin contact cellular remains, microorganisms, sebum and other materials, which can affect penetration. To overcome these structures, the penetrant has two potential routes to viable tissue:

- Transappendageal route
- Transepidermal pathway (across intact stratum corneum)

The transappendageal routes circumvent penetration through the stratum corneum and therefore are known as the shunt routes. The shunt routes include permeation through sweat glands and across the hair follicles. The relative importance of the shunt routes versus transport across the stratum corneum has been debated by researchers over the years. It is generally accepted that as the appendages occupy a fractional area for permeation of approximately 0.1%, their contribution to steady state flux of most drugs is minimal [25, 27]. This presumption has lead many penetration enhancement techniques to concentrate on increasing transport across the stratum corneum rather than via appendages [28]. However, resent investigations have shown hair follicles may represent an important target for drug delivery as they are surrounded by a close network of blood capillaries and dendritic cells [24]. In particular, hair follicles appeared to be an important reservoir for particulate carrier systems [29-31].

The route across the stratum corneum contains intercellular (through the intercellular lipid domain) and transcellular pathways (aqueous regions near the outer surface of intracellular keratin filaments) [25, 28]. Traditionally it was thought that lipophilicity of a compound dictates the partitioning behaviour into the stratum corneum; hydrophilic compounds tend to partition into the corneocyte's proteins while more lipophilic compounds into the lipid domain [32]. Based on more recent data, the intercellular route is considered to be the main passage for permeation of most of the drugs [28, 33] .

Below the stratum corneum, the intercellular tight junctions (TJ) are considered as one of the major barriers to paracellular transport, transport between or around the cells [17]. TJ structure and permeability can be regulated by many potential physiological factors, including the concentration of cyclic AMP and intercellular  $\text{Ca}^{2+}$ . By opening the TJ paracellular transport of hydrophilic compounds would be allowed [34]. In skin with normal barrier function, the role of TJ is still a subject of further investigations [14-17].

Little evidence has been found to suggest there are any active processes involved in skin permeation. It therefore seems likely that the drug transport process is controlled by simple passive diffusion [35]. Fick's first law (equation 1) can be used to analyse permeation data and can be simplified to:

$$\frac{dm}{dt} = J = \frac{DC_0 K}{h} \quad (1)$$

where J is the steady-state flux, D is the diffusion coefficient of the drug in the stratum corneum over a diffusional path length or membrane thickness (h), K is the partition coefficient between the stratum corneum and the vehicle and  $C_0$  the applied drug concentration which is assumed to be constant [28, 35]

From equation 1 the ideal properties of a drug penetrating stratum corneum can be deduced. There are:

- i) Low molecular mass, preferably less than 600 Da,
- ii) Adequate solubility in oil and water,
- iii) High but balanced K (too large may inhibit clearance by viable tissues)
- iv) Low melting point ( $<200^\circ\text{C}$ ) [27, 36].



### 3.2 Mechanisms of enhancement

For successful skin drug delivery, a topical formulation must release drugs into the stratum corneum and then from the stratum corneum into the epidermis and dermis. Several approaches have been taken to enhance drug transport across the skin. They rely either on the use of chemical penetration enhancer, novel vehicle systems (e.g. microemulsion, nanoemulsion), lipid-based delivery systems and supersaturated formulations or physical enhancement methods as iontophoresis, electroporation, ultrasound, microneedle array and others [37].

An ideal penetration enhancer would have following attributes:

- The enhancement should be immediate and unidirectional, and the duration of the effect should be specific, predictable and suitable,
- After removal of the material from the applied membrane, the tissue should immediately fully recover its normal barrier property,
- The enhancer should show no systemic or toxic effects and not irritate or damage the applied membrane surface,
- The enhancer should be physically compatible with a wide range of drugs [34].

In most cases unfortunately, the better a penetration enhancer works, the more irritating it is to the skin. For example, chemical enhancers weaken the skin barrier by either disrupting or fluidizing the lipid lamellae and/or increase the drug solubility and partitioning into the stratum corneum. Chemical permeation enhancers collectively refer to a group of compounds spread across different structural classes such as organic solvents, fatty acids, surfactants, azone, alkyl amines, dimethyl sulfoxide (DMSO) and others [4, 6, 27, 37].

Another strategy to increase drug uptake is the selection of nanosized carriers. These may be categorised as:

- Nanoparticles (polymeric nanoparticles, solid lipid nanoparticles, metallic particles, mineral particles)
- Lipid based nanoparticles (liposomes, niosomes, transferosomes, ethosomes) [1, 27, 38]

Nanosized carriers are mostly composed of physiological and biodegradable materials, which possess low cytotoxicity and low systemic toxicity. Thus, they can be used as an efficient, non-irritating enhancer through the skin [39, 40]. Particle size and distribution are very important factors in the completion of particles. Batches with wide particle size distributions have shown significant variations in drug loading, drug release, bioavailability and efficacy. Other important parameters needed to evaluate the suitability of these carrier systems are their loading capacity and entrapment efficiency [41].

### 3.3 Nanoparticles

The benefits of nanoparticles have been shown in several scientific fields, but little is known about their potential to penetrate the skin. Nanoparticles may enhance percutaneous transport into and across the skin barrier [42]. Particle penetration is most likely along two possible routes, the intercellular, following the lipids between corneocytes and the appendage, into hair follicles [30, 42]. Solid lipid nanoparticles (SLN) are composed of physiological lipids and surfactants manufactured by a high pressure homogenisation. Their application onto skin induces higher drug penetration. It has been observed that these nanoparticles diffuse into the hair follicle [40]. On the other hand, metallic nanoparticles, such as gold and iron particles, have been used for dermal penetration, and it has been determined that the smallest particles (<15 nm) penetrate deeper skin layers, whereas larger particle types (198 nm) only reach the viable epidermis. This kind of nanoparticles seem to be able to passively penetrate through the SC lipid matrix and the epidermis appendages [31,43]. In comparison, mineral nanoparticles as TiO<sub>2</sub> and ZnO with sizes between 50-500 nm, when used as sun-protector agents, remain on the skin surface and do not penetrate into the living skin [44, 45].

#### 3.3.1 Polymeric nanoparticles

The carrier technology most commonly used for drug delivery purposes is based on polymeric materials, particularly on biomaterial that offer an intrinsic biodegradability and biocompatibility. There are already several studies on drug penetration from polymeric nanoparticles that have shown a marked difference between the conventional and nanoparticulate formulations. Polymeric nanoparticles are particles of less than 100 nm diameter that can be prepared from natural or synthetic polymers [46]. Biodegradable natural polymers exploited to prepare nanoparticles are: chitosan, alginate, gelatine and pullulan. Biodegradable synthetic polymers used for nanoparticles production include poly-lactic acid (PLA) and poly-lactic-co-glycolic acid (PLGA). Nonbiodegradable polymeric nanoparticles can be applied for controlled drug delivery and also in diagnostic imaging. Examples of nonbiodegradable synthetic polymers used in drug delivery include polymethyl methacrylate (e.g.

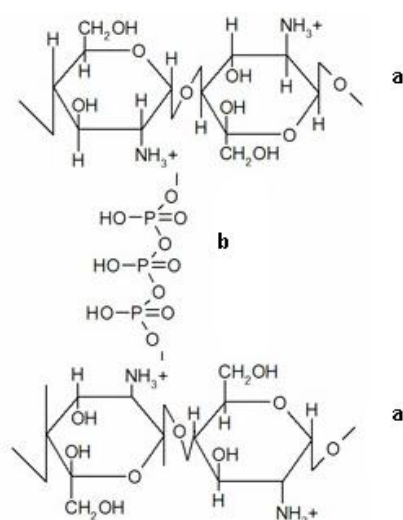
Eudragit®) while polystyrene agents have been accepted as diagnostic agents [41]. Chitosan and Eudragit EPO are the polymers used in the present theses. Although polymeric nanoparticles are undoubtedly able to enhance skin penetration, the mechanism of enhancement is still unclear. Polystyrene nanoparticles have been observed, via confocal laser scanning microscopy, to accumulate into the follicles. Interestingly, the smaller nanoparticles (20 nm) were more concentrated in the follicular openings than larger nanoparticles (190 nm), which could be due to their higher surface area. This has also been demonstrated with carriers of micrometer range. Three to ten  $\mu\text{m}$  polymeric particles selectively penetrated the follicular ducts. Particle larger than 10  $\mu\text{m}$  remained on the skin surface, while smaller than 3  $\mu\text{m}$  were randomly distributed in the hair follicles and stratum corneum [39]. More importantly, polymeric nanoparticles can increase the stability of sensitive drugs by protecting the molecules in a polymeric shell [47].

Due to its biological properties such as biocompatibility and biodegradability, chitosan (CS) has become the most widely used polymer in medical and pharmaceutical applications [48]. Chitosan is a polysaccharide composed of 2-amino-2-deoxy- $\beta$ -D-glucan combined with glycosidic linkages and has many advantages, particularly for developing micro- or nanoparticles. These include its: **i)** ability to control the release of drugs, **ii)** solubility in aqueous acidic solutions, **iii)** free amino groups available for cross-linking and **iv)** cationic nature that allows ionic cross-linking with polyanions. Different methods have been used to prepare CS particulate system (Table 1). However, selection of any of these methods depends upon the nature of the drug as well as the type of the delivery device [49].

**Table 1** Chitosan based particulate systems [49]

Type of system	Method of preparation
Microparticles	Emulsion cross-linking
	Coacervation/precipitation
	Spray-drying
	Ionic gelation
	Sieving method
Nanoparticles	Emulsion-droplet coalescence
	Coacervation/precipitation
	Reverse micellar method
	Ionic gelation

Some CS based microparticles have been already evaluated on skin in terms of wound-healing properties [49]. In the present theses the ionic gelation method was used. This method has attracted much attention because the process is very simple [49]. Micro- or nanoparticles are formed by electrostatic interaction between the positively charged chitosan (CS) chains and polyanions (Figure 5). The most extensively used polyanion is tripolyphosphate (TPP) [48].

**Figure 5** Interaction of (a) chitosan with (b) tripolyphosphate

Biocompatible chitosan-tripolyphosphate (CS-TPP) nanoparticles have been studied with regard to different therapeutic applications. They have shown excellent nasal as well as good ocular surface drug delivery [50, 51]. Furthermore, it has been found that CS-TPP nanoparticles can be used for skin gene therapy [52]. Still, compared with other nanoparticulate formulations, CS-TPP nanoparticles appear rather unexplored in relation to drug delivery via the skin.

With respect to drug delivery, positive charged amino groups of CS interact with negatively charged sites on the cell surface and also possibly with tight junctions (TJ), if nanoparticles penetrate the stratum corneum [34, 53].

Additionally, CS has good film forming properties and hence it is applied as a coating material in drug delivery formulations. CS coated micro- or nanoparticles have many advantages over uncoated particles such as improvement of drug contents, bioadhesive property and prolonged drug release properties [49]. This polymer has been investigated for stabilisation of liposomes as well as microemulsion based on lecithin. It has been observed that the coating of these lipid based nanostructures increases their stability properties [54-56].

### 3.4 Lipid based particles

One of the possibilities for increasing the penetration of drugs is the use of vesicular systems based on phospholipids. Phospholipids, dispersed in water, spontaneously form bilayer membrane vesicles (liposomes) or may act as surfactants in forming micro- or nanoemulsions [2, 57]. They have also shown to cause less irritation than chemical enhancers such as unsaturated fatty acids [58]. The advantage of phospholipids lies in their biocompatibility as they are natural components of biological membranes. Hence, phospholipids can be generally considered as safe for topical application [59].

#### 3.4.1 Liposomes

Liposomes are spherical structures that contain an aqueous core entirely enclosed by one or more concentric spheres of lipid bilayers, composed usually of natural (egg yolk or soybean lecithin) and/or synthetic lipids (e.g. dipalmitoyl-phosphatidylcholine (DPPC), dimirystoyl-phosphatidylcholine (DMPC), distearoyl-phosphatidylcholine (DSPC); but other ingredients such as cholesterol and ceramides are also possible [27, 60, 61] Liposomes are classified according to the number of bilayers and their diameter into small unilamellar vesicles (SUV, 20-100 nm), large unilamellar vesicles (LUV, > 100 nm) and multilamellar vesicles (MLV, 100 nm – 5  $\mu$ m) [41].

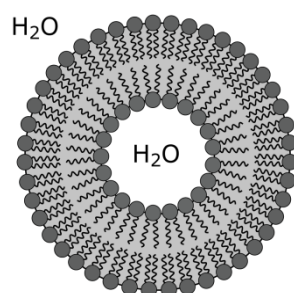


**Figure 6** Structure of an unilamellar liposome

Liposomes can be produced by a variety of conventional methods including BANGHAM, detergent depletion, ether/ethanol injection, inverted emulsion, and reverse phase evaporation. Advanced methods are including freeze drying of monophasic solution, microfluidic channel, membrane contactor, heating, supercritical fluid injection and decompression, supercritical liposome method, improved/supercritical reverse phase evaporation and depressurisation of an expanded solution into aqueous media. After production they can be modified to alter size, lamellarity and homogeneity. The most common methods for post-formation processing are sonication, extrusion and high pressure homogenization [62].

Liposomes have various benefits as drug carriers. They are biodegradable, they have low toxicity and they are able to encapsulate hydrophilic drugs within an aqueous core and a lipophilic material within the lipid phase [60, 63]. However, liposome lipids, like many biomolecules, undergo different destabilisation processes. The most common problems are: **i)** lipids may degrade by hydrolysis and oxidation and **ii)** the physical structure of liposomes may be affected by aggregation or fusion [64]. Chemical changes of liposomes can be minimised by preparing liposomes from pure lipids and by keeping the pH of liposomes close to neutral. The process of liposome fusion can be retarded by liposomes storage at low temperature and/or by increasing the viscosity of the external media [5]. As an alternative many have attempted to use biocompatible polymers (also used in our case) for the surface modification of liposomes, obtaining a stable liposomal system for application in different environments [54, 55]. Liposomes stabilisation can also be achieved through freeze-drying [5].

Due to they have a lipid bilayer, especially liposomes formed from the extracted stratum corneum lipids (ceramides, cholesterol and fatty acids), liposomes are thought to serve as a model for the skin membrane. They have been employed mainly to investigate the mechanisms of action of skin penetration enhancers and/or the changes in bilayer organisation by membrane-drug interactions [65, 66]. Because of the complexity of the skin's lipids it is common to carry out fundamental experiments (FTIR, microDSC) on well characterised phospholipid



membranes such as DPPC liposomes, which were used in the present work [25].

The potential of liposomes for delivering drugs to the skin was first reported by Mezei et al. in 1980, who showed five times greater skin delivery from the liposomes than an ointment containing the same drug concentration. In therapy of psoriasis patients vitamin-A-acid loaded liposomes showed ten times higher drug content in the skin in comparison with conventional topical formulations. Side effects, skin redness and skin brand, were likewise less presented. Minoxidil supplied liposomes also achieved good results in treatment of alopecia patients [67].

Many studies performed in the last decade showed significantly higher absorptions rates as well as greater pharmacological effects for drugs applied to the skin while entrapped in liposomes, as compared to ordinary topical applications [68, 69]. Still, the mechanism of enhanced drug uptake is not completely clear and is being intensively discussed. There are several possible mechanisms proposed: **i)** vesicles penetrate stratum corneum intact, **ii)** lipid bilayer stacks are formed on the surface of stratum corneum, **iii)** vesicles fragments penetrate into the stratum corneum and finally **iv)** the vesicles do not interact with the stratum corneum. It has been observed by freeze-fracture microscopy that intact liposomes are detected mainly in the upper cell layers of the stratum corneum, changing its lipid bilayer structure, and do not penetrate into its lower regions [70]. This is in accordance with findings of electron microscopy studies on humans, where liposomes do not penetrate deeper than the horny layer [71]. Other studies have noted phospholipids, as the major component of liposomal systems, can easily get integrated with the skin lipids. They maintain desired hydration conditions to improve drug penetration through the stratum corneum and localisation in the skin layers [72-74]. Moreover, recent studies have established the facility of liposomes for drug transport into the pilosebaceous units (hair follicles and sebaceous glands) via the follicular route [75]. Thus, it is possible that liposomes either find their way into a shunt or accumulate in one of the wider space between corneocytes clusters where

they can interact with skin lipids or they merge into extended lipidic structures on the skin surface and indirectly influence skin permeation [28, 33].

Moreover, many drugs have properties which are far from ideal for dermal applications. They may have poor solubility, rapid metabolism, instability under physiological conditions or unfavourable biodistribution leading to toxicities. Liposomes can increase therapeutic indications for a variety of drugs by alleviating these characteristics [76]. Furthermore, inclusion of drugs in supramolecular systems, such as liposomal systems, is an approach of growing interest with regard to the problem of light-sensitive drugs. Liposome matrices represent one of the most studied photo-protective carriers and successful results have been reported in many studies [77].

## 4 Specific topics

### 4.1 Chitosan-TPP nanoparticles as a possible skin drug delivery system for aciclovir with enhanced stability

Amra Hasanovic<sup>1</sup>, Martin Zehl<sup>2</sup>, Gottfried Reznicek<sup>2</sup>, Claudia Valenta<sup>1</sup>

J. Pharm. Pharmacol. 2009, 61: 1609-1616

<sup>1</sup>University of Vienna, Department of Pharmaceutical Technology and Biopharmaceutics

Faculty of Life Sciences

Althanstrasse 14

1090 Vienna

AUSTRIA

<sup>2</sup>University of Vienna, Department of Pharmacognosy,

Althanstrasse 14, A-1090 Vienna, Austria

Corresponding Author: Claudia Valenta

Department of Pharmaceutical Technology and Biopharmaceutics

Faculty of Life Sciences

Althanstrasse 14

1090 Vienna

AUSTRIA

E-mail: [claudia.valenta@univie.ac.at](mailto:claudia.valenta@univie.ac.at)

Tel: +43 1 4277 55 410

Fax: +43 1 4277 955

**Abstract**

The aim of the present study was to create a skin delivery system based on chitosan-tripolyphosphate (CS-TPP) nanoparticles for aciclovir with enhanced chemical stability. In standard diffusion experiments using Franz-type diffusion cells, reasonable skin permeability dependent on the particle sizes and CS content was shown. Using the method of ionotropic gelation with TPP the nanoparticles were formed spontaneously. Two different sizes of aciclovir-loaded CS-TPP nanoparticles were characterised on their physicochemical properties in terms of zeta potential, particle sizes and polydispersity index (PDI). The larger the nanoparticle, having a higher CS content, the better the aciclovir permeation through porcine skin. Additional differential scanning calorimetry (DSC) studies showed a remarkable decrease of the typical transition temperature indicating an interaction between skin lipid bilayer and CS-TPP nanoparticles. Moreover, the chemical stability of aciclovir was significantly increased by the nanoparticle system. After the observation period of five weeks, aciclovir incorporated into nanoparticles had undergone photo-oxidation to a significantly lower extent compared to a pure aqueous solution. This degradation product of aciclovir is analysed by using LC-MS, and its identity established.

**Keywords:** CS-TPP nanoparticles, skin diffusion, aciclovir, DSC, LC-MS

## 1 Introduction

Chitosan (CS) is a natural cationic polymer obtained by deacetylation of chitin using chemical or enzymatic reactions. In the usual sense, CS is chitin with more than 40% deacetylation. From the chemical point of view, it is a polycationic copolymer consisting of  $\beta$ -(1-4)-linked glucosamine and N-acetylglucosamine units. Chitosan is increasingly favoured in various fields of drug delivery for its biological properties such as biocompatibility and non-toxicity. CS is metabolised by lysozyme which is able to crack the CS into smaller units [1, 2]. Furthermore, CS possesses mucoadhesive, wound healing and antimicrobial properties [3, 4]. The presence of reactive amino groups means that CS can be modified easily to create micro- and nanoparticles or porous hydrogels [5]. Chitosan microparticles and nanoparticles have been made by chemical cross-linking with different kinds of polyanions such as glycyrrhetic acid, polyaspartic acid and other oppositely charged molecules, yielding controlled-drug-release formulations with less toxicity [6, 7]. One of the most extensively used polyanions is tripolyphosphate (TPP). The interaction of CS with TPP leads to the formation of biocompatible nanoparticles. The cross-linking density, crystallinity and hydrophilicity of cross-linked CS allow modulation of drug release and extend its range of potential applications in drug delivery [8].

Given the successful use of CS-TPP nanoparticles through different barriers in recent years, we investigated whether they may also be useful for skin drug delivery [9, 10]. The aims of the present study were therefore to create a CS-TPP drug delivery system for acyclovir (model drug), to improve its permeability through the skin, to enhance the chemical stability of acyclovir by incorporation into CS-TPP nanoparticles and to characterise physicochemical properties of the new delivery systems.

## **2 Materials and Methods**

### **2.1 Materials**

Chitosan (CS, < 500 kDa) in powdered form was a gift from Syntapharm (Mülheim, Germany). The degree of deacetylation was determined by NMR as 95% [11]. Tripolyphosphate (TPP) and methanol were supplied by Sigma-Aldrich Chemie GmbH (Steinheim, Germany). Acyclovir was purchased from Fagron GmbH (Barsbüttel, Germany).

### **2.2 Preparation of CS-TPP nanoparticles**

CS-TPP nanoparticles were prepared using ionotropic gelation between positively charged amino groups of chitosan and negatively charged TPP, as reported previously by Krauland and Alonso [12]. Briefly, 0.1 g or 0.2 g CS were dissolved in 100 ml of distilled water in the presence of 1 N HCl (which is essential to achieve protonation of amino groups) under magnetic stirring over night at room temperature [13]. TPP aqueous solution (1 ml of about 0.7 mg/ml) was added to various volumes of 0.1% CS and of 0.2% CS solution under gentle stirring at room temperature in order to obtain different CS : TPP (v/v) ratios. The final ratios were obtained by mixing 1 ml TPP with 3.5 ml 0.1% CS or 3.5 ml 0.2% CS solution for 10 min. The nanoparticles were formed spontaneously and were then concentrated by centrifugation at 24,562×g for 30 min, at 25°C in glycerol bed (10 µl glycerine). The supernatants were discarded and the CS-TPP nanoparticles were resuspended in 100 µl purified water [12]. The final pH value of all tested solutions was between 5.3 and 5.5.

For incorporation of aciclovir into the CS-TPP nanoparticles, aciclovir was directly dissolved in the acidic CS solution in a concentration of 0.45 mg/ml, following by the procedure described above.

### **2.3 Effect of pH on formation of nanoparticles**

The pH of the CS solution was adjusted to values in the range from pH 3.5 to 6.5 by addition of 0.1 mM HCl or NaOH. Different batches of CS-TPP nanoparticles were produced by combining these CS solutions with aqueous TPP solutions. Each experiment was repeated five times.

## **2.4 Physicochemical characterisation of nanoparticles**

The particle size and polydispersity index (PDI) of the CS-TPP nanoparticles were determined by photon correlation spectroscopy; the zeta potential was determined by electrophoretic mobility using a Zetasizer Nano ZS (Malvern Instruments, Malvern, United Kingdom). For particle size analysis and determination of the electrophoretic mobility, samples were diluted with filtered distilled water (n=5).

For calculation of the yield, a fixed volume of the nanoparticles was centrifuged at  $24,562\times g$  for 40 min at room temperature without a glycerol bed. The supernatants were discarded and the microtubes containing the centrifugates were frozen at  $-20^{\circ}\text{C}$ . The samples were then freeze-dried at  $-30^{\circ}\text{C}$  for 3 h followed by  $-55^{\circ}\text{C}$  overnight. After thawing the samples for 2 h at room temperature, the yield was determined by calculating the ratio of the actual weight and theoretical weight of the nanoparticles (n=3) [14].

## **2.5 Determination of loading capacity and encapsulation efficiency**

To determine loading capacity (LC) and encapsulation efficiency (EE), aciclovir-loaded nanoparticles were isolated by centrifugation as described above. The amount of unbound aciclovir in the discarded supernatant was detected by HPLC using a diode array detector (series 200 LC Perkin Elmer, Norwalk, CT, USA) at a wavelength of 252 nm. Briefly, supernatants (n=3) were diluted with 1 N  $\text{CaCl}_2$  and then centrifuged at  $24\,562\times g$  for 10 min in order to precipitate disturbing polymer residue (we confirmed that the treatment with 1 N  $\text{CaCl}_2$  did not decrease the aciclovir concentration significantly). After filtration (0.45  $\mu\text{m}$  pore size), 20  $\mu\text{l}$  of the supernatant were injected onto the system using an autosampler (series 200 Perkin Elmer). Separation was achieved using a C-18 RP column (Nucleosil 100-5, 250 mm x 4 mm, Macherey-Nagel, Düren, Germany) at  $40^{\circ}\text{C}$ . The mobile phase consisted of methanol/water 10/90 [15]. The flow rate was maintained at 1.0 ml/min. The acyclovir concentration used to construct the calibration curve was in the range from 0.05 to 10  $\mu\text{g/ml}$  (n=7). The loading capacity and encapsulation efficiency of acyclovir were calculated as described below:

Loading capacity =

$$\frac{\text{Total amount of drug} - \text{amount of unbound drug}}{\text{Nanoparticles weight}} \times 100$$

Encapsulation efficiency =

$$\frac{\text{Total amount of drug} - \text{amount of unbound drug}}{\text{Total amount of drug}} \times 100$$

## ***2.6 Physicochemical stability of nanoparticles at room temperature***

The different batches of CS-TPP nanoparticles with and without aciclovir were stored at room temperature for an observation period of six weeks. Particle size and zeta potential were monitored weekly using Zetasizer (Nano ZS; Malvern Instruments, Malvern, United Kingdom) (n=5).

## ***2.7 Chemical stability of aciclovir in nanoparticles***

The chemical stability of aciclovir incorporated into CS-TPP nanoparticles was compared with its stability in aqueous solution. The concentrations of aciclovir in CS-TPP nanoparticles and in control sample were the same. The samples were stored in Eppendorf tubes under day-light exposure at air-conditioned room temperature (approximately 22°C). HPLC analysis (described in 2.4) was performed weekly for five weeks (n=3). To characterise the main degradation product of aciclovir, an aqueous solution of aciclovir, that had been stored in an Eppendorf tube under day-light exposure at room temperature for 2 weeks, was analyzed by LC-MS. The analysis was performed on an UltiMate 3000 RSLC-series system (Dionex, Germering, Germany) coupled to an electrospray ionization-3D-ion trap mass spectrometer (ESI-IT-MS) (HCT, Bruker Daltonics, Bremen, Germany). Ten µl of the sample were loaded onto a C-18 RP column (Nucleosil 100-5, 250 mm x 4 mm, Macherey-Nagel) and eluted into the orthogonal ESI source using a 10 min linear gradient of 0-10% methanol (HPLC grade) in 5 mM ammonium acetate pH 7.5 at a flow of 1.0 ml/min. The mass spectrometer was operated in an automated data-dependent acquisition (DDA) mode where each MS scan (m/z 50-400, average of five spectra) was followed by a MS/MS scans (m/z 15-300, average of five spectra, isolation window 4 Th)



of the most intense precursor ion. Helium was used as collision gas and the fragmentation amplitude was 0.40 V in positive ion mode and 0.60 V in negative ion mode. Source parameters were as follows: capillary voltage: 4.0 kV, nebulizer ( $N_2$ ): 60 psi dry gas flow ( $N_2$ ): 12 l/min and dry temperature: 365°C. For comparison, freshly prepared aqueous solutions of aciclovir and guanine hydrochloride were also analyzed. The aciclovir solution containing the degradation product was re-analyzed after incubation with 1 M HCl overnight at 37°C.

### **2.8 *In vitro* permeation studies**

In vitro permeation studies with porcine abdominal skin were performed as reported previously [16]. About 1 ml of aciclovir-loaded 0.1% or 0.2% CS-TPP nanoparticles was applied to the skin surface. Prior to quantification the permeated samples were diluted with 1 N  $CaCl_2$ , centrifuged at 17 586×g for 6 min and filtered (pore size 0.45  $\mu$ m). Each batch was quantified in quadruplicate following the HPLC method described above. As a control we used aciclovir dissolved in water at the same concentration as in the nanoparticles (0.45 mg/ml). The pH value of all applied solutions was approximately 5.4.

### **2.9 Differential Scanning Calorimetry**

Differential Scanning Calorimetry (DSC) profiles of thawed and additionally dabbed porcine epidermis were obtained using a Perkin-Elmer DSC 7 differential scanning calorimeter. Sliced skin samples (1 cm<sup>2</sup>) were impregnated for 14 hours with 2 ml water (control), 0.1% CS-TPP or 0.2% CS-TPP nanoparticle formulations. The sample weight was in the range of 17-20 mg. The samples were placed in aluminium pans and sealed hermetically, then heated from 30 to 120°C at a constant rate of 5°C/min under a continuous flow of dry nitrogen. Transition temperatures reported from all thermograms are taken from peak maxima values and from onset temperatures. Gravimetric analysis of untreated skin samples prior to DSC experiments showed average water content of about 55.7% (w/w)  $\pm$  1.44. Treated samples absorbed about 10% (w/w)  $\pm$  7 of used impregnation.

### **2.10 Statistical data analysis**

Results are given as means  $\pm$  S.D. of at least three experiments. Data were exported to the Graph Pad Prism statistics software. Analysis groups consisted of independent mean values; the Gaussian distribution of the data was verified using the Kolmogorov-Smirnov test. Statistical analysis was performed by one-way analysis of variance followed by Dunnet's or Tukey's post-hoc tests. Values of loading capacity and encapsulation efficiency and results of diffusion studies were analysed using paired Student's t-test.  $P < 0.05$  was considered significant.

## **3 Results**

### **3.1 Preparation and physicochemical characterisation of pure nanoparticles and pH effect**

CS-TPP nanoparticles were established only with particular chitosan : TPP ratios (Table 1). Regarding to entanglement of chitosan chains with TPP to form particles, a higher content of chitosan resulted in formation of significantly larger nanoparticles [17]. This was confirmed by our results (Table 1).

Table 2 shows that the pH of chitosan solution influenced the particle size and PDI values. The size of the nanoparticles did not show any significant difference in the pH range from 3.5 to 4.9. From pH 4.9 to 6 they showed remarkable swelling behaviour ( $P < 0.05$ ), and aggregated at pH values higher than 6, where chitosan became completely uncharged. The interaction between chitosan and TPP was completely destroyed at pH values lower than 3.5, resulting in the dissolution of nanoparticles. The zeta potential of successfully produced nanoparticles was positive, in the range 22 to 30 mV.

**Table 1** Physicochemical properties of chitosan–tripolyphosphate nanoparticles prepared with different ratios (v/v) of 0.1% and 0.2% chitosan and tripolyphosphate

CS/TPP ratio (v/v)	Mean particle size (nm)	Polydispersity index	Zeta Potential (mV)	Yield (%)
0.1%chitosan				
2/1	Precipitation	-		
3/1	Precipitation	-		
4/1	Precipitation	-		
4,5/1	350 ± 20	0.14-0.24	+31± 2	25.9 ± 1.1
5/1	368 ± 20*	0.21-0.23		
5,5/1	390 ± 10*	0.22-0.27		
6/1	510 ± 10*	0.22-0.27		
0.2%chitosan				
2/1	Precipitation	-		
3/1	Precipitation	-		
4/1	450 ± 50	0.4-0.52		
4.5/1	634 ± 38**	0.12-0.24		
5/1	600 ± 50**	0.6-0.8	+31 ± 2	40.3 ± 0.8
5.5/1	700 ± 10**	0.9-1.0		
Values are means ± SD from at least five experiments. Significantly larger particles compared with the *4.5/1 or **4/1 nanoparticles (Dunnet's test)				

**Table 2** Effect of pH on nanoparticles distribution of 0.1% chitosan-tripolyphosphate nanoparticles

pH	Mean particle size (nm)	Polydispersity index	Zeta potential (mV)
3.5	330 ± 20	0.27-0.29	29 ± 1.1
4	360 ± 21	0.25-0.26	21 ± 2.1
4.5	367 ± 14	0.28-0.30	21 ± 0.5
4.9	350 ± 21	0.14-0.24	31 ± 2.0
5.5	500 ± 23*	0.40-0.44	22 ± 1.0
6	520 ± 26*	0.35-0.36	22 ± 0.8
6.5	Precipitation	-	-
Values are means ± SD from five experiments. *P < 0.05 (Tukey's test)			

### **3.2 Encapsulation of aciclovir within nanoparticles and physicochemical properties of nanoparticles**

Incorporation of aciclovir, a poorly soluble substance (1.3 mg/ml in water at 25°C) into the CS-TPP nanoparticles was optimised by dissolving aciclovir directly in the CS solution at a concentration of 0.45 mg/ml. However, an increase in particle size with higher CS content did not result in significantly higher loading capacity or higher encapsulation efficiency (Table 3).

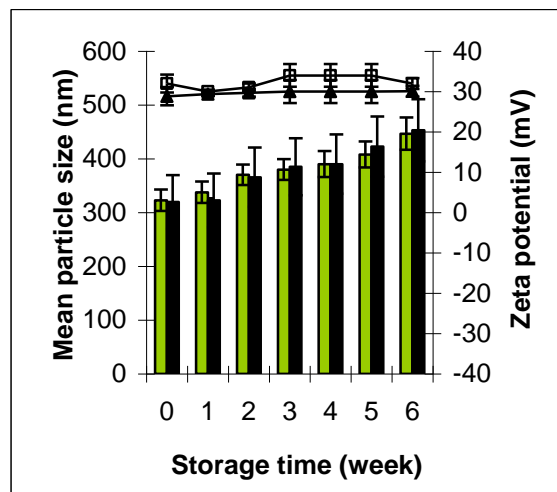
**Table 3** Physicochemical characteristics of acyclovir-loaded 0.1% and 0.2% chitosan-tripolyphosphate nanoparticles

	0.1% chitosan	0.2% chitosan
CS/TPP ratio (v/v)	4.5/1	4.5/1
Mean particle size (nm)	380 ± 50	703 ± 15
Polydispersity index	0.11-0.21	0.23-0.28
Zeta potential (mV)	+30 ± 3	+27 ± 3
Loading capacity (%)	6.02 ± 0.4	6.23 ± 0.5
Encapsulation efficiency (%)	13.56 ± 0.6	14.06 ± 0.4
Yield (%)	32.6 ± 2.3	44.5 ± 2
The total amount of acyclovir is 0.45 ± 0.05 mg/ml of CS-TPP solution. Values are means ± SD of at least five experiments		

### **3.3 Physicochemical stability of nanoparticles at room temperature**

CS-TPP nanoparticle formulations were unstable at room temperature in terms of mean particle size. Cuna et al. explained this property as colloidal system tendency to aggregate [14].

Our experiments verified this fact for both 0.1% CS (Figure 1) and 0.2% CS (Figure 2) nanoparticles. Aggregation ability was much higher in 0.2% CS-TPP nanoparticles, showing a significant increase in particle size compared with 0.1% CS-TPP nanoparticles at each weekly measurement. The particles size of the latter was significantly increased after five weeks. The incorporation of aciclovir into 0.2% CS-TPP nanoparticles resulted in physical break down after two weeks (Figure 2). However, we successfully incorporated acyclovir into formulation with 0.1 chitosan; the physical stability of these did not decrease within six weeks, evidenced by the stabile zeta potential (Figure 1).



### Mean particle size

### Zeta potential

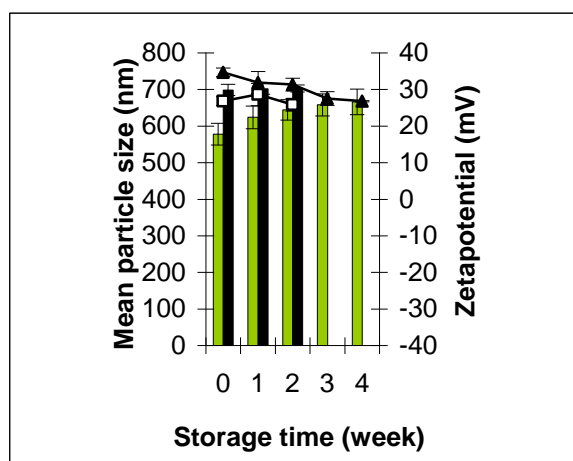
■ Control nanoparticles

▲ Control nanoparticles

■ Aciclovir-loaded nanoparticles

□ Aciclovir-loaded nanoparticles

**Figure 1** Comparison of the physicochemical stability of 0.1% chitosan-tripolyphosphate nanoparticles with and without aciclovir. Values are means  $\pm$  SD of at least five experiments



### Mean particle size

### Zeta potential

■ Control nanoparticles

▲ Control nanoparticles

■ Aciclovir-loaded nanoparticles

□ Aciclovir-loaded nanoparticles

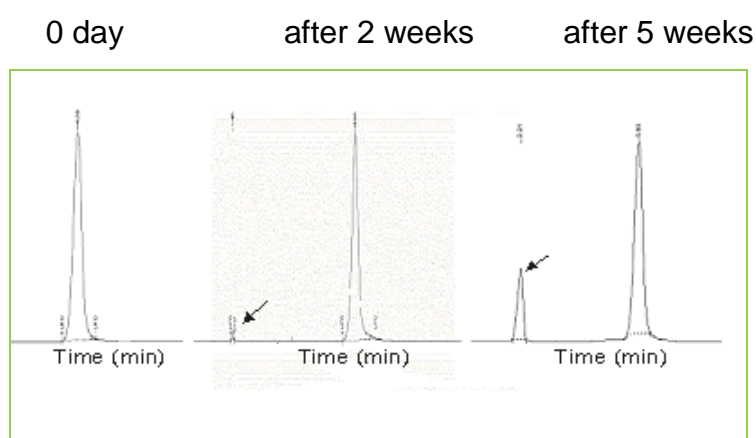
**Figure 2** Comparison of the physicochemical stability of 0.2% chitosan-tripolyphosphate nanoparticles with and without aciclovir. Values are means  $\pm$  SD of at least five experiments

### 3.4 Chemical stability of aciclovir in nanoparticles

Aciclovir is an important antiviral drug used in the treatment of many types of herpes infections. However, it has been found that aciclovir degraded under exposure to light, oxidants, temperature and in different solvents [15].

The HPLC analysis clearly shows a degradation product at a retention time of about 1.5 min (Figure 3), which is in agreement with literature data, where the photolytic degradation of aciclovir to a non-identified chromophoric compound is explained [15].

(a)



(b)

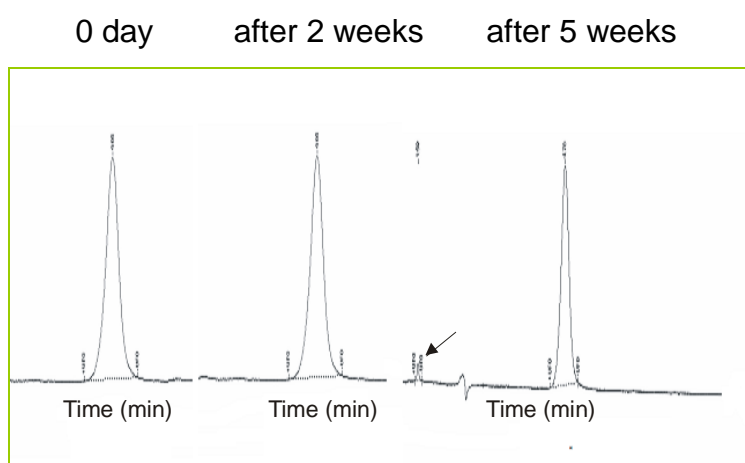


**Figure 3** Chromatograms showing the photolytic degradation of aciclovir in (a) water and (b) chitosan–tripolyphosphate nanoparticles after 2 and 5 weeks

According to the results of the degradation studies under daylight exposure at room temperature, 12% of aciclovir in CS-TPP nanoparticles degraded after 5 weeks whereas 12% of aciclovir in water had decomposed within two weeks.

To further characterise the photolytic degradation product of aciclovir, LC-MS analysis was performed. Whereas in freshly prepared aqueous solutions only aciclovir (3) is detected (Figure 4a), a prominent degradation product (1) is formed following two weeks' light exposure at room temperature (Figure 4b). This degradation product is different from guanine (2), which is formed by acid-catalysed hydrolytic cleavage of the N<sub>9</sub>-linked (2-hydroxyethoxy) methyl-chain upon incubation with 1 M HCl overnight at 37°C (Figure 4c). The molecular weight of the degradation product (239.1 Da) is 14 Da higher than the mass of aciclovir (225.1 Da). From the comparison of the MS<sup>2</sup> spectra of aciclovir (Figure 5a and 5c) and the degradation product (Figure 5b and 5d), it can be concluded that photooxidation of the 2-hydroxyethoxy-group has occurred. Since the mass spectrometric response of both species in positive and negative ion mode is comparable, the photooxidation product is likely to be 9-((2-hydroxyacetyl) methyl) guanine.

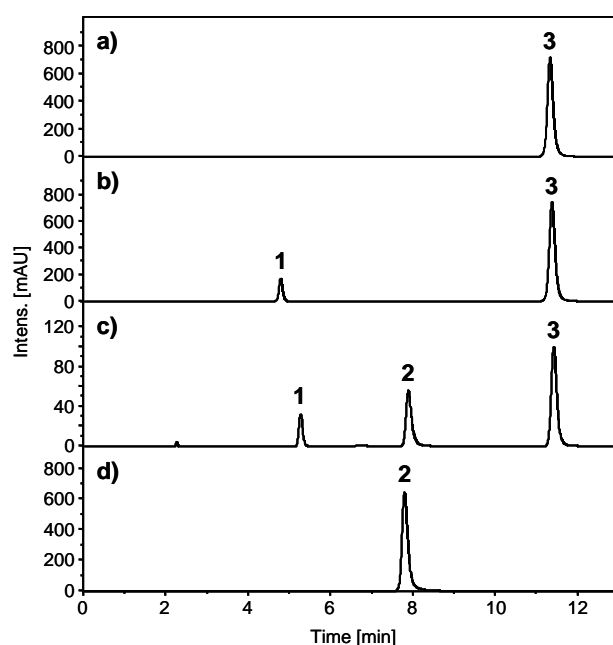


**Figure 4** HPLC chromatograms (UV trace at 252 nm) of aqueous solutions of (a) freshly prepared aciclovir, (b) aciclovir stored in an eppendorf tube under light exposure at room temperature for 2 weeks and (c) additionally incubated with 1 M HCl overnight at 37°C, and (d) guanine hydrochloride.

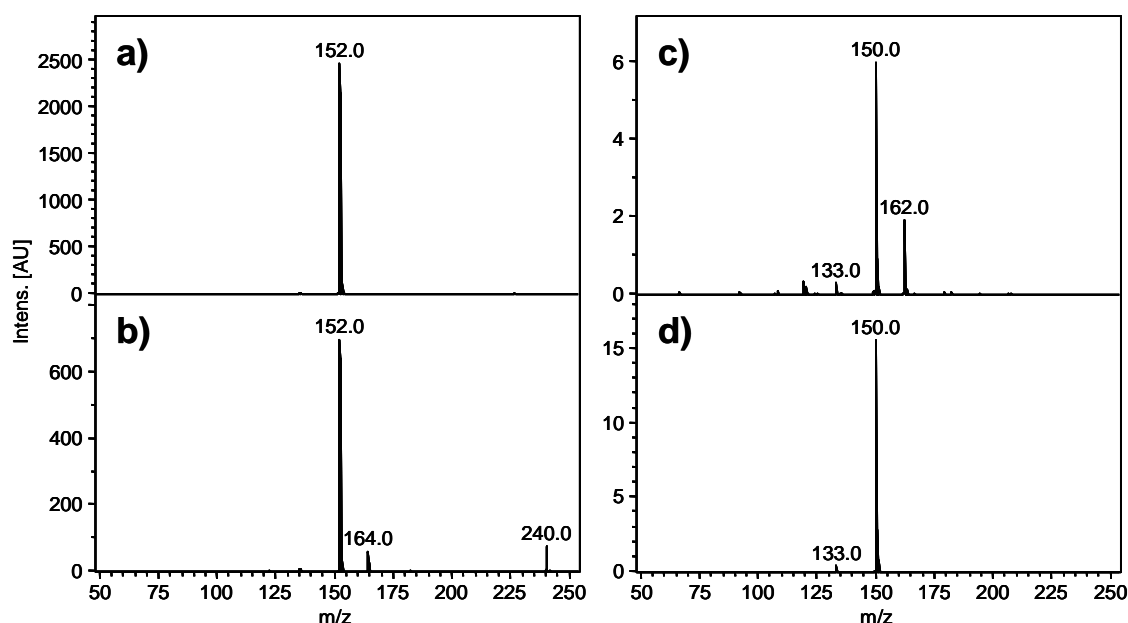


**Figure 5** Electrospray ionisation–3D-ion-trap mass spectrometry spectra of (a) the  $[M+H]^+$  ion of aciclovir ( $226.0 \rightarrow$ ), (b) the  $[M+H]^+$  ion of the photo-oxidation product ( $240.0 \rightarrow$ ), (c) the  $[M-H]^-$  ion of aciclovir ( $224.1 \rightarrow$ ), and (d) the  $[M-H]^-$  ion of the photo-oxidation product ( $238.1 \rightarrow$ ). The main product ions of aciclovir originate from the elimination of the Ng-linked (2-hydroxyethoxy) methyl-chain ( $m/z$  152.0 or  $m/z$  150.0) and the elimination of the 2-hydroxyethoxy group ( $m/z$  162.0). In the case of the photo-oxidation product, the fragment ions are interpreted as the elimination of Ng-linked (2-hydroxyacetyl) methyl-chain ( $m/z$  152.0 or  $m/z$  150.0) and the elimination of the 2-hydroxyacetyl group ( $m/z$  164.0).

### 3.5 Skin diffusion

In the *in vitro* permeation studies, two different sizes of CS-TPP nanoparticles containing aciclovir were applied to porcine skin for 48 hours. The permeation of aciclovir was proportional to the nanoparticle size, regulated by the amount of chitosan. In other words, larger particle sizes improved the aciclovir diffusion through the epidermis. The permeation of aciclovir from larger particles was about 1.5-fold higher than from smaller nanoparticles (Figure 6;  $P < 0.05$ ).

The diffusion profile of aciclovir from CS-TPP nanoparticles through the epidermis was biphasic, reflecting the initial fast partition of aciclovir close to the nanoparticle surface followed by a slower diffusion of the drug entrapped inside the nanoparticle matrix [17]. According to Figure 6, aciclovir permeation after 8 hours was approximately 50% of the drug penetration over 48 hours. Therefore, it might be possible to control the penetration of aciclovir by the use



of CS-TPP nanoparticles.

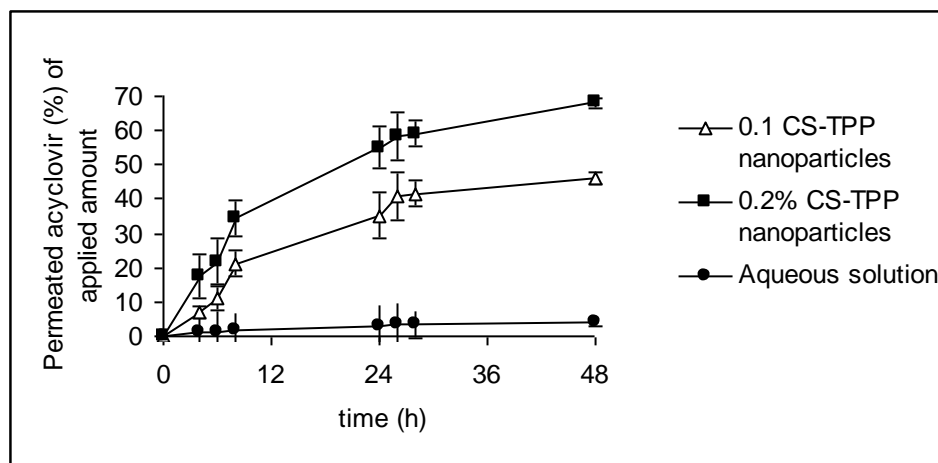


**Figure 6** Comparison of aciclovir permeation through porcine skin from different chitosan–tripolyphosphate nanoparticles and aciclovir aqueous solution. Graph shows means  $\pm$  SD of four experiments.

### 3.6 Differential scanning calorimetry studies

DSC thermograms of porcine skin with and without treatment are shown in Figure 7. It is obvious that the different impregnation types resulted in different thermograms. Porcine skin has one endothermic peak at around 78°C which corresponds to intracellular lipid layers [18-20].

Treatment of the skin with water as well as with nanoparticle formulations resulted in a shift to significantly lower temperatures ( $P < 0.05$ ). The maximum transition temperature (peak maxima value) was shifted from 78°C for untreated skin to 66.5°C after treatment with 0.2% CS-TPP nanoparticles (Figure 7). Moreover, a comparison of skin impregnated with 0.2% and 0.1% CS-TPP nanoparticles still indicates a significant shift in onset temperature ( $P < 0.05$ ) (Table 4).

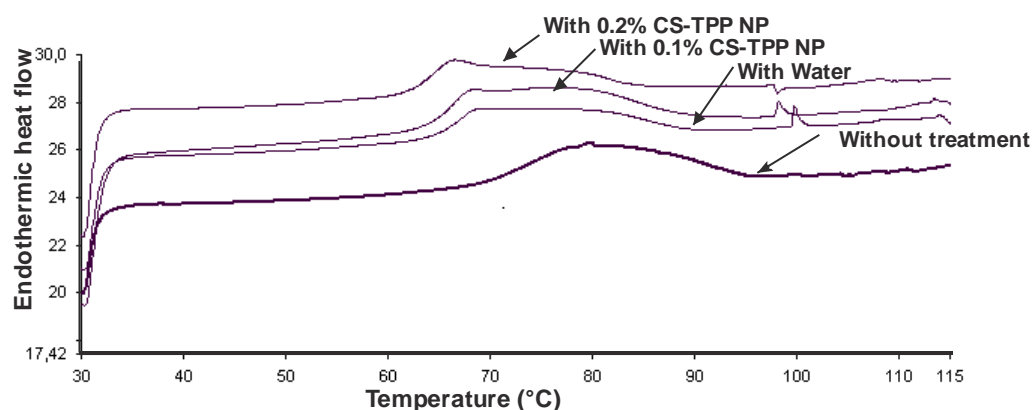


**Figure 7** Thermograms of porcine skin

**Table 4** Thermal changes after impregnation of porcine skin with water, 0.1% or 0.2% CS-TPP nanoparticles

Impregnation	skin-water (control)	skin-0.1% CS-TPP nanoparticles	skin-0.2% CS-TPP nanoparticles
Peak (°C)	69.82 ± 0.89	67.60 ± 0.53	66.49 ± 0.28
Onset (°C)	64.82 ± 0.14	63.93 ± 0.31*	62.09 ± 0.25*
Values are means ± SD ( n>4); *P < 0.05 vs. control (Tukey's test)			

#### 4 Discussion

CS–TPP nanoparticles were formed by means of electrostatic interaction between the positively charged  $\text{-NH}_2$  groups of chitosan in acidic medium (pH 4.9) and negatively charged phosphate and hydroxide groups of TPP aqueous solution, which compete with each other to interact with  $\text{-NH}_3^+$  sites of chitosan [8]. The nanoparticles were positively charged over the chitosan : TPP ratio used, reflecting the excess of chitosan amino groups, which may be favourable for drug delivery because of enhanced interaction with negatively charged groups on the skin surface. It was also evident that the pH of the chitosan solution plays a significant role in the formation of nanoparticles [6]. As a consequence of these results, we chose for all further studies nanoparticles produced using chitosan solution at a pH 4.9 that gives optimal PDI and zeta potential values. The chemical stability of aciclovir was improved by incorporation into the nanoparticles, implying successful protection by the nanoparticulate system.

The better permeation of aciclovir from larger nanoparticles could be explained by the interaction of positively charged nanoparticles with anionic components of the

epithelial cell surface. The surface charge density of larger nanoparticles may cause a stronger interaction with the cell surface, resulting in better permeation of aciclovir [21].

Moreover, the DSC measurements indicate a possible interaction between CS–TPP nanoparticles and the skin lipids. Interestingly the larger nanoparticles interacted more strongly, showing lower onset temperature.

## **5 Conclusion**

These studies demonstrate that CS-TPP nanoparticles significantly improve the chemical stability of aciclovir, and the possible use of CS-TPP nanoparticles for delivering aciclovir to the skin. Skin diffusion data showed significantly improved permeation of aciclovir from nanoparticles.

The ratio of CS to TPP is the most important factor for formation of reproducible nanoparticles. The size of nanoparticles depends on the chitosan content. Increasing the initial chitosan input in the formulation resulted in a larger mean particle diameter. The higher the chitosan content the higher the aciclovir skin permeation.

## References

1. Kim K.W. *et al.* Antimicrobial activity of native chitosan, degraded chitosan and O-carboxymethylated chitosan. *J Food Protect* 2003; 66:1495-1498.
2. Luessen H.L. *et al.* Mucoadhesive polymers in peroral peptide drug delivery. VI. Carbomer and chitosan improve the intestinal absorption of the peptide drug buserelin in vivo. *Pharm Res* 1996; 13: 1668-1672.
3. Liu X.F. *et al.* Antibacterial action of chitosan and carboxymethylated chitosan. *J Appl Polym Sci* 2001; 79: 1324-1335.
4. Felt O. *et al.* Chitosan as Tear substitute: A wetting agent endowed with antimicrobial efficacy. *J Ocul Pharmacol Ther* 2000; 16: 261-270.
5. Bodnar M. *et al.* Synthesis and study of cross-linked chitosan-n-poly (ethyleneglycol) nanoparticles. *Biomacromolecules* 2006; 7: 3030- 3036.
6. Zheng Y. *et al.* Preparation, characterisation and drug release in vitro of chitosan-glycyrrhetic acid nanoparticles, *J Pharm Sci* 2006; 95: 181-191.
7. Zheng Y. *et al.* Nanoparticles based on the complex of chitosan and polyaspartic acid sodium salt: Preparation, characterisation and the use for 5-flurouracil deliver. *Eur J Pharm Biopharm* 2007; 67: 621-631.
8. Bhumkar D.R., Pokharkar V.B. Studies of effect of pH on cross-linking of chitosan with sodium tripolyphosphate: A technical note. *Pharm Sci Tech* 2006; 7: 1-11.
9. Enriquez de Salamanca A. *et al.* Chitosan nanoparticles as a potential drug delivery system for the ocular surface: Toxicity, uptake mechanism and in vivo tolerance. *Invest Ophtamol Vis Sci* 2006; 47: 1416-1425.
10. Fernandez-Ursuno R. *et al.* Enhancment of nasal absorption of insulin using chitosan nanoparticles. *Pharm Res* 1999; 16: 1576-1581.
11. Kählig H. *et al.* Chitosan-glycolic acid: a possible matrix for progesterone delivery into skin. *Drug Dev Ind Pharm* 2009; 1: 1-6
12. Krauland A.H., Alonso M.J. Chitosan/cycodextrin nanoparticles as macromolecular drug delivery system. *Int J Pharm* 2007; 340: 134-142.
13. Messai I., Delair T. Cationic biodegradable particles: Comparison of one or two step processes. *Colloids Surf* 2006; A 278: 188-196.

14. Cuna M. *et al.* Development of phosphorylated glucomannan-coated chitosan nanoparticles as nanocarriers for protein delivery. *J Nanosci Nanotechnol* 2006; 6: 1-9.
15. Sinha V.R. *et al.* Stress studies on aciclovir. *J Chromatogr Sci* 2007; 45: 319-324.
16. Höller S., Valenta C. Effect of selected fluorinated drugs in a "ringing" gel on rheological behaviour and skin permeation. *Eur J Pharm Biopharm* 2006; 66: 120-126.
17. Zgoneanu I.G. *et al.* Nanoparticles with entrapped alpha tocopherol; synthesis, characterisation and controlled release. *Nanotechnology* 2008; 19: 1-8
18. Sadeghi A.M. *et al.* Permeation enhancer effect of chitosan and chitosan derivatives: Comparison of formulations as soluble polymers and nanoparticulate systems on insulin absorption in Caco-2 cells. *Eur J Pharm Biopharm* 2008; 70: 270-278.
19. Lopez-Ceravantes M. *et al.* Chemical enhancer for the absorption of substances through the skin: Laurocapram and its derivatives. *Drug Dev Ind Pharm* 2006; 32(3): 267-286.
20. Golden M.G. *et al.* Stratum corneum lipid phase transition and water barrier properties. *Biochemistry* 1986; 26: 2382-2388.
21. Hirvonene J. *et al.* Mechanism and reversibility of penetration-enhancer action in the skin. A DSC study. *Eur J Pharm Biopharm* 1994; 40: 81-85.
22. Smith J. *et al.* Effect of chitosan on epithelial cell tight junctions. *Pharm Res* 2003; 21: 43-49.

#### **4.2 Improvement of physicochemical parameters of DPPC liposomes and increase of skin permeation of aciclovir and minoxidil by addition of cationic polymers**

Amra Hasanovic<sup>1</sup>, Caroline Hollick<sup>1</sup>, Kerstin Fischinger<sup>1</sup>, Claudia Valenta<sup>1</sup>  
Eur. J. Pharm. Biopharm. 2010, 75: 148-153

University of Vienna, Department of Pharmaceutical Technology and  
Biopharmaceutics  
Faculty of Life Sciences  
Althanstrasse 14  
1090 Vienna  
AUSTRIA

Corresponding Author: Claudia Valenta  
Department of Pharmaceutical Technology and Biopharmaceutics  
Faculty of Life Sciences  
Althanstrasse 14  
1090 Vienna  
AUSTRIA  
E-mail: [claudia.valenta@univie.ac.at](mailto:claudia.valenta@univie.ac.at)  
Tel: +43 1 4277 55 410  
Fax: +43 1 4277 9554

**Abstract**

1,2-Dipalmitoyl-sn-glycero-3-phosphatidylcholine (DPPC) liposomes were prepared by high pressure homogeniser and coated with two cationic polymers, chitosan (CS) and for the first time Eudragit EPO (EU), respectively. Compared to the control liposomes, the polymeric liposomes showed greater physicochemical stability in terms of mean particles size and zeta potential at room temperature. In the present study, aciclovir and minoxidil have been used as hydrophilic and hydrophobic candidates. In the presence of the drugs the polymeric liposomes still showed constant particle size and zeta potential. Influences of polymers and model drugs on thermotropic phase transition of DPPC liposomes were studied by micro differential scanning calorimetry (microDSC). The influences on configuration of DPPC liposomes were investigated by Fourier transform infrared spectroscopy (FTIR). According to DSC results cationic polymers had a stabilising effect, whereas aciclovir and minoxidil changed the physical properties of the DPPC bilayers by influencing the main phase transition temperature and erasing the pre-transition. The investigation of C=O stretching bands of DPPC at  $1736\text{ cm}^{-1}$  in FTIR spectra showed that aciclovir has strong hydrogen bonding with C=O groups of DPPC, whereas carbonyl groups were free in minoxidil presence. Moreover, the coating of liposomes with CS or EU led to higher skin diffusion for both drugs. This could be explained as an effect of positive charged liposomes to interact stronger with skin negatively charged surface and their possible interactions with structures below the stratum corneum.

**Keywords:** DPPC, Chitosan, Eudragit EPO, DSC, FTIR, Flux

## 1 Introduction

Liposomes are spherical structures consisting of one or more phospholipid bilayers enclosing an aqueous core and are generally produced from highly purified phospholipids extracted from soy oil or egg yolk or synthetic phospholipids what is the case in the current study. They have been claimed to improve transdermal drug delivery and can be used as a model for the skin membrane [1]. Plenty of studies reported that liposomes were able to improve skin permeation of various entrapped drugs through the major barrier stratum corneum [2]. The possible mechanism of liposomes action on distribution of drug through the skin is probably through the fusion of the vesicles either in the channel-like structures between corneocytes or in hair follicles or by their disintegration of extended lipid structures [3, 4].

However, liposomes have some limitations. They generally adhere to each other and after certain time fuse to form larger vehicles. As an alternative many attempts to use biocompatible polymers for the surface modification of liposomes, obtaining a stabile liposomal system for application in different environments [2, 5]. Polymers are macromolecule constituents of many useful materials that, depending on their molecular structures, can have different properties. At present, polymers have applications in many different areas including their use as chromatographic material, carriers for molecules and cells, for modulation of living processes, changing properties of food products and for the development of many pharmaceutical applications. Moreover, during the last decade, the use of polymers in drug delivery has been extensively studied.

Chitosan (CS), the natural, bioadhesive, biocompatible and biodegradable polymer seems to be an optimal candidate to be combined to liposomes. As a cationic biopolymer it showed the ability to improve skin compatibility of skin formulations and enhancing effect on the penetration of cosmetic ingredients and drugs [6, 7]. Eudragit EPO (EU) was selected for liposome coating as a second cationic polymer. This polycation, insoluble at physiological pH exhibited mucoadhesive characteristics [8]. Moreover, Alasino et al. showed additional membrane destabilising properties and increase in efflux of doxorubicin from liposomes [9]. In some studies EU has been regarded as a



dissolution modifier. Some other groups used EU's ability to improve the solubility of drugs with low aqueous solubility [10].

In the present study three main goals should be achieved:

- i) To increase physicochemical stability of DPPC liposomes in terms of mean particles size and zeta potential in the presence and in the absence of the drugs by coating with the two cationic polymers, CS and EU, respectively.
- ii) To characterise interactions of the polymers and the drugs with DPPC by microDSC and FTIR.
- iii) To improve skin permeation of aciclovir and minoxidil by coating with CS and EU, respectively.

## 2 Materials and methods

### 2.1 Materials

1,2-Dipalmitoyl-sn-glycero-3-phosphatidylcholine was kindly donated by Lipoid (Switzerland). The product was synthetic Lipoid PC 16:0/16:0. The content of phosphatidylcholine was at least 99 % related to the dry weight. Eudragit EPO (EU, <150 kDa, structure is presented in Figure 1) was kindly provided by Evonik (Darmstadt, Germany). Chitosan (CS, < 500 kDa) in the powder form was a gift from Syntapharm (Mülheim, Germany). The degree of deacetylation was determined by NMR with 95% [11]. Aciclovir was purchased from Fagron GmbH (Barsbüttel, Germany) and minoxidil from Kwizda (Vienna, Austria). All other chemicals used in this study were of analytical reagent grade and were used as received without any further purification.

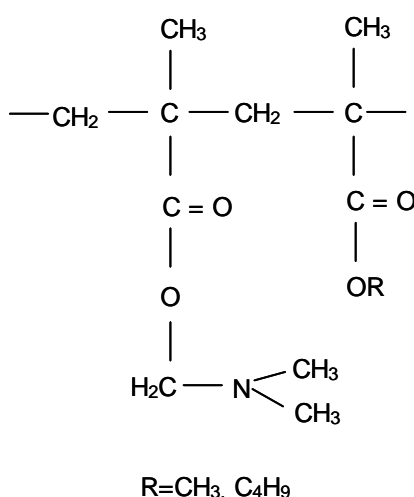


**Figure 1** Structure of Eudragit EPO

### 2.2 Liposomes preparation

DPPE liposomes were prepared according to a modified method of Brandl et al as described recently [12, 13]. Briefly, the phospholipid powder was dispersed in distilled water at 60°C in the concentration of 5% (w/w) and magnetically stirred until the powder was completely dissolved and thoroughly mixed using an ultra-turax (Omni 500, Glendale, Canada). Afterwards the dispersion was homogenised with a high-pressure homogeniser (EmulsiFlex-C3, Avestin, Canada) for 16 times at approximately 1100 bar. The liposomes were kept at

4°C over night and diluted with purified water 1:1 the day after and characterised in terms of mean particles size and PDI. An aqueous dispersion of 2% (w/w) of aciclovir and minoxidil, respectively, was added to already formed liposomes in the volume ratio 1:1 and afterwards mechanically stirred over night at 50°C.

### ***2.3 Chitosan and Eudragit EPO (EU) coated liposomes***

The already prepared liposomes described above were coated with CS and EU by adding a polymer solution in volume ratio 1:1 and mechanically stirred for 30 min. Firstly, different polymer concentrations in 0.01 M acetate buffer ranging between 0.125% and 1% (w/w) were used. The final products were determined in terms of mean particles size, zeta potential and polydispersity index (PDI). For incorporation of aciclovir and minoxidil the liposomes with the lowest polymer concentration of 0.125% were used. The drugs were suspended in this polymer solution in a concentration of 2% (w/w) and further diluted with aqueous liposomes 1:1 (v/v) and stirred over night at 50°C.

### ***2.4 Analysis of size and zeta potential of DPPC liposomes***

The particle size and polydispersity index (PDI) of liposomes were analysed by photon correlation spectroscopy, and the zeta potential was determined by electrophoretic mobility using a Zetasizer Nano ZS (Malvern Instruments, Malvern, United Kingdom). To observe changes of the particles size (expressed in Z-average size) and zeta potential, the batches of pure and coated liposomes with and without drugs were stored at room temperature over a period of twenty weeks. Samples were diluted 1:30 with filtered 0.1 mM acetate buffer obtaining conductivity of <0.05 ms/cm and monitored weekly (n=5). Each sample was measured three times in 13 runs (sampling time was 5 and 15 min).

### ***2.5 Micro-Differential scanning calorimetry (microDSC) studies***

Differential thermal analysis was performed using a Setaram III micro-calorimeter as previously reported [14]. Samples of pure and polymer coated liposomes, prepared as described above, were scanned. We also performed

consecutive runs for each sample [14]. The measurement conditions were: 1.00°C/min for the scanning rate over the temperature range of 15-65°C, using purified water as reference.

Thermal transitions were calculated using Setsoft 2000 Setaram software. After baseline subtraction, raw power data were converted to molar heat capacity data. Baselines were fitted to the pre-transition and main transition regions using a linear baseline function so that transition temperatures and enthalpies of reaction could be calculated for each lipid concentration.

## **2.6 Fourier transform infrared (FTIR) spectroscopy**

Spectra were recorded on a FTIR spectrophotometer (model: Tensor 27, Bruker Optics, Ettlingen, Germany) with a photovoltaic MCT detector at a temperature of 25°C. The samples of pure and coated DPPC liposomes with and without aciclovir or minoxidil were scanned on Bio-ATR II tool against demineralised water as a reference (n=5).

## **2.7 In vitro aciclovir and minoxidil permeation**

In vitro permeation studies with porcine abdominal skin were carried out as previously reported [15]. Briefly, about 0.5 ml of aciclovir and minoxidil loaded liposomes with and without coating was respectively applied to the skin surface. The diffusion studies were performed for 10 hours with a phosphate buffer (pH 7.4) as an acceptor medium, where the samples were taken every two hours and measured by HPLC. The HPLC analysis of permeated drug (n=4) was carried out on a C-18 RP column (Nucleosil 100-5, 250 mm x 4 mm, Macherey-Nagel, Düren, Germany) at 40°C. The mobile phase consisted of methanol/water 10/90 for aciclovir and methanol/water/acetic acid 75/25/1 for minoxidil [16, 17]. The aciclovir and minoxidil concentrations used to construct the calibration curve were in the range from 0.005 to 0.25 mg/ml (n=6). The flow rate was maintained at 1.00 ml/min and the injection volume was 20 µl. Furthermore, the flux  $J$  [ $\mu\text{gcm}^{-2}\text{h}^{-1}$ ] of both drugs in each preparation was calculated from the slope of the linear portion of the cumulative amount permeated through the porcine skin per unit area versus time plot.

## **2.8 Statistical data analyses**

Results of current studies are expressed as the means  $\pm$  SD of four (skin diffusion studies) and of five experiments (particle size, zeta potential, microDSC, FTIR). Data were exported to the GraphPad Prism statistics software package. Analysis groups consisted of independent mean values and the Gaussian distribution of the data was verified using the Kolmogorov-Smirnov test. Statistics were performed using one-way ANOVA with post-hoc Dunnet's test. The values of diffusion studies were analysed with nonparametric t-test. P values of  $< 0.05$  were considered significant.

## **3 Results and Discussion**

Different preliminary experiments were necessary to optimize the preparation process with ultra-turax and following high pressure homogenisation. On the one hand we figured out that the temperature of 60°C during the suspension of DPPC was very important to obtain reproducible liposomes. On the other hand the ultra-turax speed and mixing time had only a small effect on particle size. According to a previous investigation sixteen cycles in homogenizer at 1100 bar were suitable for liposomes production [12, 13]. By monitoring the particle size, zeta potential and PDI using light scattering the unloaded liposomes at room temperature have shown constant mean particle size, PDI and zeta potential for seven weeks (Table 1,  $P > 0.05$ ). After this time period, the size and PDI started to increase significantly ( $P < 0.05$ ), indicating merging of liposomes that could lead to phase separation [18]. Therefore physical stability is a general problem with liposomes. As an alternative CS and EU, two cationic polymers were employed to improve the stability. As seen in Table 2a and 2b the higher the polymer content the larger the particles size, for both polymers ( $P < 0.05$ ). That was the result of the chemical interaction which probably involves hydrogen bonding between the polymer and the phospholipid head groups on the vehicles surface [7]. The charge of liposomes increased from approximately 0.50 to 40 mV with addition of CS or EU. The values of zeta potential were almost in the same range independent of the amount of polymer (Table 2a and 2b). Finally, both polymers caused stable particle size and uniformly PDI values for longer time that could be explained by the positive

charge of the particles. Immediately after production, the coated liposomes had a zeta potential between 30 and 40 mV and stayed significantly longer unaltered than control liposomes (Table 1). The EU coated liposomes have not shown any changes within twenty weeks ( $P < 0.05$ ), while the zeta potential of CS coated liposomes decreased after eight weeks and after sixteen weeks liposomes started to aggregate resulting in larger particles size and PDI values (Table 1).

**Table 1** Physicochemical stability of DPPC, CS DPPC and EU-DPPC liposomes expressed in mean particle size as Z-average (MPS), poly dispersity index (PDI) and zeta potential (ZP).

Week	DPPC			CS DPPC**			EU DPPC**		
	MPS(nm)±SD	PDI±SD	ZP(mV)±SD	MPS(nm)±SD	PDI±SD	ZP(mV)±SD	MPS(nm)±SD	PDI±SD	ZP(mV)±SD
Start	88.15±1.00	0.18±0.01	0.51 ± 0.79	97.11 ±1.80	0.27±0.02	40.72±0.79	95.66±1.54	0.20±0.01	36.64±0.60
1	87.22±0.71	0.17±0.01	0.50 ± 0.85	97.64±0.48	0.23±0.01	40.72±0.80	95.99±0.52	0.20±0.01	31.58±1.56
2	89.03±1.29	0.16±0.01	1.02 ± 0.26	102.80±1.3	0.25±0.01	47.84±1.18	94.53±0.68	0.19±0.01	32.69±0.39
3	85.97±0.42	0.16±0.01	2.00 ± 0.80	101.72±1.6	0.24 0.01	40.76±1.28	99.38±1.40	0.21±0.01	34.90±0.84
4	86.04±0.44	0.16±0.01	3.23 ± 0.91	102.58±0.9	0.24±0.01	40.70±1.99	99.42±1.02	0.20±0.01	38.94±1.50
5	84.51±0.48	0.13±0.01	2.12 ± 0.89	98.65±0.75	0.23±0.01	36.19±1.11	97.95±1.43	0.20±0.01	38.11±1.31
6	88.89±2.07	0.15±0.01	1.15 ± 0.79	98.55±0.62	0.23±0.01	40.72±1.03	97.97±1.30	0.21±0.01	40.86±4.37
7	90.82±1.28	0.17±0.01	2.18 ± 0.59	97.73±0.39	0.22±0.01	41.99±3.06	98.54±1.39	0.21±0.01	39.26±0.54
8	100.72±1.9*	0.21±0.02	1.12 ± 0.36	95.21±1.22	0.22±0.01	28.29±0.25	98.29±1.50	0.21±0.01	37.94±1.05
9	173.29±2.0*	0.43±0.01	0.13 ± 0.19	95.25±1.3	0.21±0.01	28.29±0.22	94.94±0.81	0.21±0.01	35.66±0.93
10	-	-	-	96.58±0.99	0.22±0.01	23.00±1.16	95.51±0.53	0.21±0.01	36.42±1.16
12	-	-	-	97.65±0.75	0.23±0.01	23.50±3.05	94.78±0.68	0.22±0.01	34.19±0.65
14	-	-	-	98.55±0.62	0.23±0.01	24.10±3.12	95.84±0.34	0.22±0.01	33.63±0.74
16	-	-	-	120.05±0.4*	0.41±0.05	10.00±0.50	93.70±0.94	0.22±0.01	31.44±1.67
18	-	-	-	-	-	-	94.05±1.50	0.24±0.02	31.96±0.66
20	-	-	-	-	-	-	95.51±0.53	0.21±0.01	36.42±1.16

Values are means ± SD n=5

\*Significantly larger particles compared with the start (Dunnet's test).

\*\*Amount of polymer is 0.125%

**Table 2a** Mean particles size as Z-average (MPS), poly dispersity index (PDI) and zeta potential (ZP) of CS-DPPC liposomes

CS (%)	MPS (nm) $\pm$ SD	PDI $\pm$ SD	ZP (mV) $\pm$ SD
0	88.15 $\pm$ 1.00	0.18 $\pm$ 0.01	0.51 $\pm$ 0.79
0.125	97.11 $\pm$ 0.48*	0.23 $\pm$ 0.01	40.72 $\pm$ 0.79
0.25	108.67 $\pm$ 0.64*	0.25 $\pm$ 0.01	42.09 $\pm$ 0.75
0.5	139.87 $\pm$ 0.51*	0.28 $\pm$ 0.01	40.81 $\pm$ 1.38
1.0	157.99 $\pm$ 2.70*	0.32 $\pm$ 0.04	41.41 $\pm$ 2.26

Values are means  $\pm$  SD n=5  
 \*Significantly larger particles compared with the 0% (Dunnet's test)

**Table 2b** Mean particles size as Z-average (MPS), poly dispersity index (PDI) and zeta potential (ZP) of EU-DPPC liposomes

EU (%)	MPS (nm) $\pm$ SD	PDI $\pm$ SD	ZP (mV) $\pm$ SD
0	88.15 $\pm$ 1.00	0.18 $\pm$ 0.01	0.51 $\pm$ 0.79
0.125	95.66 $\pm$ 1.54*	0.20 $\pm$ 0.01	36.64 $\pm$ 0.60
0.25	98.42 $\pm$ 1.00*	0.18 $\pm$ 0.01	38.07 $\pm$ 2.13
0.5	100.51 $\pm$ 1.30*	0.16 $\pm$ 0.01	35.98 $\pm$ 0.96
1.0	105.08 $\pm$ 1.31*	0.14 $\pm$ 0.01	32.00 $\pm$ 2.92

Values are means  $\pm$  SD n=5  
 \*Significantly larger particles compared with the 0% (Dunnet's test)

Microbial growth could not be detected in the polymer containing preparation compared to the control DPPC liposomes, which were microbial affected after two weeks.

As model substances, aciclovir and minoxidil were suspended into the described DPPC liposomes and into the coated DPPC liposomes without influencing significantly ( $P > 0.05$ ) their particles size, immediately after production (comparing start values of Table 1 with Table 3 and Table 4). However, after two weeks of storage aciclovir caused the significant growth of particles and PDI values. In contrast to this minoxidil preparations were stabile for eight weeks (Table 4). Moreover, an addition of the polymers CS or EU induced a higher stabilization effect in all liposome preparations, independent of the model drug (Table 3 and 4). Furthermore, in Table 3 and 4, zeta potential increased in DPPC liposomes by addition of the drugs, while in coated liposomes with minoxidil this was significantly lowered. In the case of aciclovir the zeta potential decreased after one week. These results might be suggesting

drugs association with the lipid bilayer [19].

**Table 3** Mean particles size as Z-average (MPS), poly dispersity index (PDI) and zeta potential (ZP) of DPPC formulations with 1% (w/w) aciclovir

Aciclovir			
Week	MPS (nm) $\pm$ SD	PDI $\pm$ SD	ZP (mV) $\pm$ SD
DPPC			
0	84.48 $\pm$ 5.21	0.14 $\pm$ 0.02	8.84 $\pm$ 2.10
1	81.10 $\pm$ 4.49	0.12 $\pm$ 0.02	5.04 $\pm$ 0.29
2	82.54 $\pm$ 4.64	0.13 $\pm$ 0.02	6.25 $\pm$ 2.30
3	127.53 $\pm$ 3.80*	0.36 $\pm$ 0.10	5.21 $\pm$ 1.02
CS DPPC			
0	99.78 $\pm$ 0.28	0.19 $\pm$ 0.01	38.00 $\pm$ 2.79
1	90.06 $\pm$ 4.86	0.19 $\pm$ 0.01	23.80 $\pm$ 4.49
2	97.81 $\pm$ 4.65	0.16 $\pm$ 0.01	20.11 $\pm$ 3.45
5	98.15 $\pm$ 4.00	0.17 $\pm$ 0.01	23.06 $\pm$ 2.62
7	94.85 $\pm$ 1.17	0.19 $\pm$ 0.01	16.84 $\pm$ 1.40
8	126.40 $\pm$ 3.84*	0.25 $\pm$ 0.03	17.46 $\pm$ 1.49
10	135.00 $\pm$ 2.20*	0.27 $\pm$ 0.02	17.39 $\pm$ 1.09
EU DPPC			
0	95.92 $\pm$ 4.10	0.15 $\pm$ 0.01	37.81 $\pm$ 2.81
1	97.00 $\pm$ 4.53	0.16 $\pm$ 0.02	41.83 $\pm$ 3.95
2	97.35 $\pm$ 3.83	0.16 $\pm$ 0.02	34.76 $\pm$ 9.01
5	94.55 $\pm$ 4.36	0.17 $\pm$ 0.01	28.42 $\pm$ 2.08
7	93.57 $\pm$ 3.84	0.19 $\pm$ 0.02	20.88 $\pm$ 3.62
8	130.60 $\pm$ 5.20*	0.25 $\pm$ 0.03	20.10 $\pm$ 2.22
10	132.12 $\pm$ 3.80*	0.24 $\pm$ 0.03	20.50 $\pm$ 2.52
Values are means $\pm$ SD n=5			
*P < 0.05 vs. week 0 (Dunnet's test)			



**Table 4** Mean particles size as Z-average (MPS), poly dispersity index (PDI) and zeta potential (ZP) of DPPC formulations with 1% (w/w) minoxidil

Week	Minoxidil		
	MPS (nm) $\pm$ SD	PDI $\pm$ SD	ZP (mV) $\pm$ SD
DPPC			
0	84.41 $\pm$ 5.95	0.16 $\pm$ 0.04	4.58 $\pm$ 0.32
1	84.02 $\pm$ 5.67	0.14 $\pm$ 0.03	3.96 $\pm$ 0.97
2	84.28 $\pm$ 4.87	0.13 $\pm$ 0.03	4.73 $\pm$ 0.48
5	84.51 $\pm$ 4.48	0.14 $\pm$ 0.03	4.10 $\pm$ 0.67
8	94.67 $\pm$ 4.57	0.22 $\pm$ 0.03	4.85 $\pm$ 1.66
9	120.50 $\pm$ 5.01*	0.23 $\pm$ 0.04	3.90 $\pm$ 1.23
CS DPPC			
0	94.97 $\pm$ 4.23	0.16 $\pm$ 0.03	10.80 $\pm$ 1.37
1	96.73 $\pm$ 3.87	0.13 $\pm$ 0.02	10.51 $\pm$ 0.39
2	96.76 $\pm$ 3.96	0.14 $\pm$ 0.03	11.41 $\pm$ 0.57
5	96.32 $\pm$ 3.85	0.14 $\pm$ 0.02	15.62 $\pm$ 8.43
8	96.18 $\pm$ 3.06	0.15 $\pm$ 0.02	11.06 $\pm$ 0.89
10	94.83 $\pm$ 3.51	0.14 $\pm$ 0.03	12.87 $\pm$ 1.29
12	97.33 $\pm$ 2.20	0.12 $\pm$ 0.02	11.64 $\pm$ 1.07
16	96.53 $\pm$ 5.02	0.14 $\pm$ 0.05	12.60 $\pm$ 1.50
EU DPPC			
0	94.65 $\pm$ 4.33	0.13 $\pm$ 0.02	23.84 $\pm$ 5.77
1	93.94 $\pm$ 4.89	0.14 $\pm$ 0.02	22.80 $\pm$ 0.35
2	95.76 $\pm$ 4.89	0.13 $\pm$ 0.01	23.96 $\pm$ 1.42
5	94.60 $\pm$ 4.87	0.14 $\pm$ 0.02	23.06 $\pm$ 2.87
8	94.83 $\pm$ 3.91	0.16 $\pm$ 0.04	20.29 $\pm$ 2.90
10	95.05 $\pm$ 2.59	0.14 $\pm$ 0.03	20.90 $\pm$ 1.51
12	95.50 $\pm$ 3.56	0.18 $\pm$ 0.02	16.10 $\pm$ 0.90
16	101.10 $\pm$ 1.26	0.20 $\pm$ 0.03	16.30 $\pm$ 0.50
Values are means $\pm$ SD n=5			
*P < 0.05 vs. week 0 (Dunnet's test)			

Further investigations to clarify and explain the stabilizing effect of polymers and possible association of the drugs with the lipid bilayer should be performed. Two well established biophysical techniques, microDSC and FTIR were chosen for this purpose.

DPPC liposomes display typical thermotropic phase behaviour with a pre-transition endotherm near  $38.4 \pm 0.25^\circ\text{C}$  and the main endotherm near  $41.4 \pm 0.05^\circ\text{C}$ , which corresponds to the gel-to-liquid crystalline ( $P\beta' \rightarrow L\alpha$ ) phase

transition (Table 5). The smaller pre-transition temperature, reflecting the lamellar to rippled gel ( $L\beta' \rightarrow P\beta'$ ) transition, has been generally attributed to the surface structure of the vehicle and is related to rotations of the phospholipid head groups or transformation in the lamellar structure and changes in the hydrocarbon chain packing [13]. In the present study, as seen in Table 5, an addition of CS and EU could not induce any significant changes in the pre and main transition temperature. However, comparing CS and EU DPPC liposomes with DPPC liposomes heating curves, the pre transition onset temperature shifted significantly to a higher temperature, pointing to the interaction with the polar region of the phospholipid bilayer (Table 5). This could mean that DPPC molecules get anchored to polymeric chains through interaction between their head groups, and the specific functional groups of polymer by electrostatic interaction. Moreover the hydroxyl groups of DPPC may interact with the hydroxyl groups of polymers through hydrogen bonding, stabilizing the lamellar structure of the liposomes what is in coherence with the increased physicochemical stability of coated liposomes [20, 21]. Furthermore, the pre transition enthalpy is reduced with increased CS or EU content, confirming the possibility of their interaction with the liposomes polar domain and the interfering with tilting of phospholipid acyl chains (Table 5) [22, 23]. Additionally, the enthalpy values of main transition temperature increased significantly in the presence of polymers (Table 5), what may be also approving an electrostatic interaction between DPPC and polymers. De Oliveira Tiera et al. also suggesting that hydrophobic interactions may induce the CS incorporation into the lipid bilayer [24].

Interestingly the addition of the drug resulted in disappearance of the pre transition temperature, whereas the main phase transition temperature was significantly raised by aciclovir and significantly lowered by minoxidil, ( $P < 0.05$ ), (Table 5). This could be described as the substances ability to interact with the surface and the phospholipid bilayer [22]. However, the addition of the drugs increases the enthalpy main transition significantly confirming the interaction with liposomes membrane. In the second and third subsequent scans main transition peak and enthalpy remain constant. This means that there are no further lipid interactions with the drugs [14].

**Table 5** Transition temperature and enthalpy values of DPPC liposomes, DPPC with 0.125 % (w/w) CS or EU and DPPC with 1% (w/w) aciclovir or minoxidil

	$T_{\max}$ (°C)	Linear Onset (°C)	Enthalpy (J/M)
DPPC	38.4 ± 0.30 pre transition 41.4 ± 0.10 main transition	36.5 ± 0.60 40.1 ± 0.10	1193 ± 121 30600 ± 430
0.125%CS DPPC	38.7 ± 0.01 pre transition 41.4 ± 0.03 main transition	37.9 ± 0.03* 40.1 ± 0.20	166 ± 10* 53000 ± 484*
1.00%CS DPPC	38.8 ± 0.01 pre transition 41.5 ± 0.01 main transition	38.1 ± 0.02 40.2 ± 0.01	102 ± 6* 54202 ± 469
0.125%EU DPPC	38.7 ± 0.06 pre transition 41.4 ± 0.01 main transition	37.9 ± 0.03* 40.1 ± 0.02	145 ± 30* 51766 ± 967*
1.00%EU DPPC	38.9 ± 0.05 pre transition 41.5 ± 0.02 main transition	38.2 ± 0.01* 40.4 ± 0.04	65 ± 10* 53254 ± 419
Aciclovir DPPC	41.9 ± 0.10* main transition	40.3 ± 0.01	54967 ± 200
Minoxidil DPPC	40.7 ± 0.04* main transition	39.4 ± 0.01	54829 ± 832
Values are means ± SD n=5			
*P < 0.05 vs. DPPC (Dunnet's test)			

An additional biophysical method is FTIR spectroscopy in aqueous systems that can be used to analyze interactions on the molecular level. With this technique, it is possible to see subtle changes in the configuration of the lipid assemblies by analyzing the frequency and the bandwidth changes of the vibrational modes. For this purpose the position of the symmetric and antisymmetric CH<sub>2</sub> bands at 2800-3000 cm<sup>-1</sup> and C=O stretching mode at 1736 cm<sup>-1</sup> of DPPC were chosen to compare different liposomal formulations [25].

In a first set of experiments by addition of polymers no shift of the acyl bands at 2800-3000 cm<sup>-1</sup> could be seen in DPPC liposomes implying a stabilization of configuration and dynamics of the bilayer. In order to analyze the interaction of CS and EU with the glycerol backbone near the head group of the phospholipids the C=O stretching band was analyzed. In contrast to previous published studies the C=O band at 1736 cm<sup>-1</sup> does not shift by addition of

solely CS or EU [5]

In Figure 2 and 3 is clearly seen that this characteristic band of DPPC, arising from the ester group vibrations was shifted significantly to lower wave numbers in the presence of aciclovir and to higher wave numbers in the presence of minoxidil ( $P < 0.05$ , Dunnet's test).

For all formulations with aciclovir, the lower frequency values suggests that hydrogen bonding may occur between the C=O groups of DPPC and either with  $\text{NH}_2$  or OH groups of aciclovir [25-27]. Whereas, the higher frequency values for all of minoxidil formulations, indicates no evidence of hydrogen bonding, instead there are free carbonyl groups in the system [27]. Interestingly, this negative and positive shifting of the C=O band is more pronounced in the presence of polymers (Figure 2 and 3).

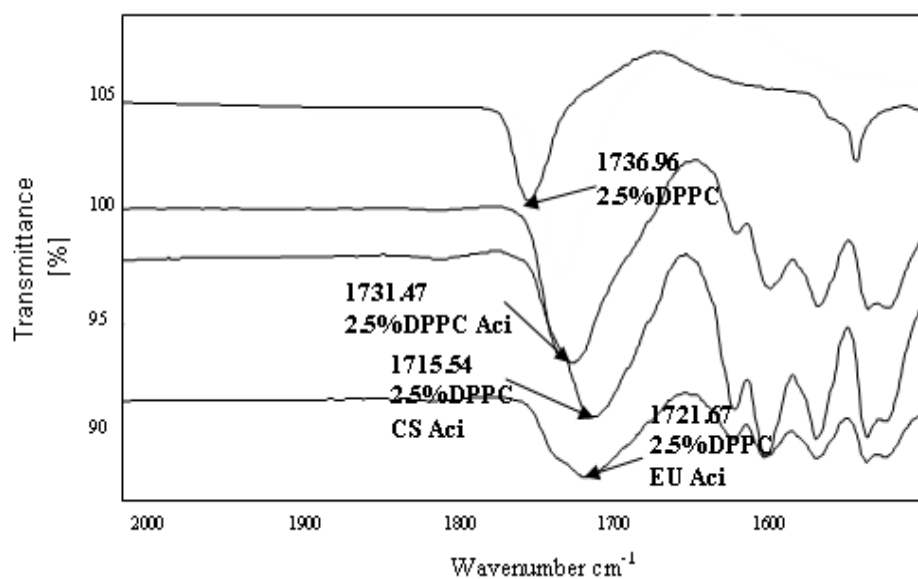


**Figure 2** FTIR transmission spectra of DPPC (control), DPPC with aciclovir (aci), CS DPPC and EU DPPC with aciclovir (aci) (as indicated with arrows) (n=5)

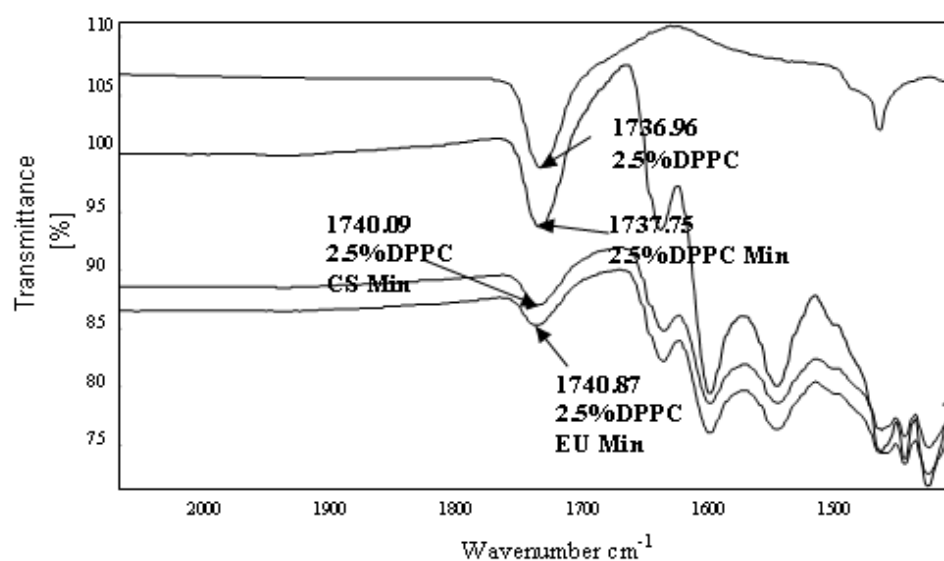


**Figure 3** FTIR transmission spectra of DPPC (control), DPPC with minoxidil (min), CS DPPC and EU DPPC with minoxidil (min) (as indicated with arrows) (n=5)

In the third part of this work, diffusion studies on porcine skin were performed to see whether the confirmed interaction between DPPC liposomes and polymers could influence the skin permeation of model drugs. As seen in Figure 4 and 5, used polymers increased the skin permeation of both model drugs significantly.

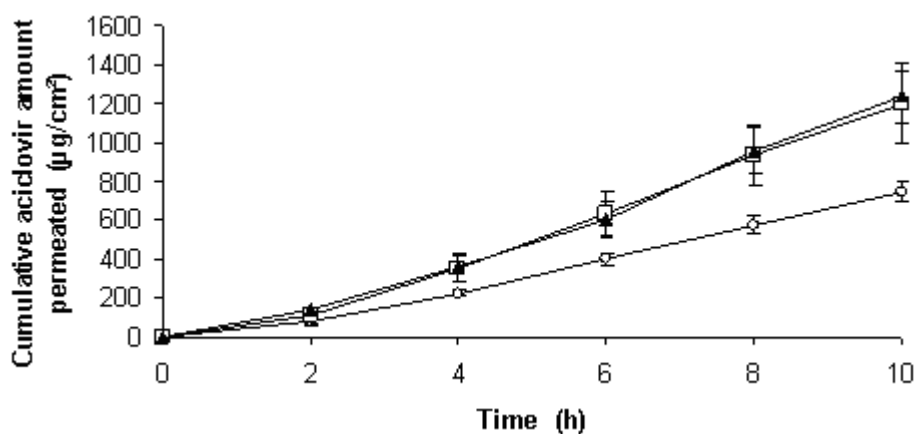


**Figure 4** Comparison of aciclovir permeation through porcine skin from different liposomal formulations (means  $\pm$  SD n=4): -▲- EU coated liposomes; -□- CS coated liposomes; -○- DPPC liposomes

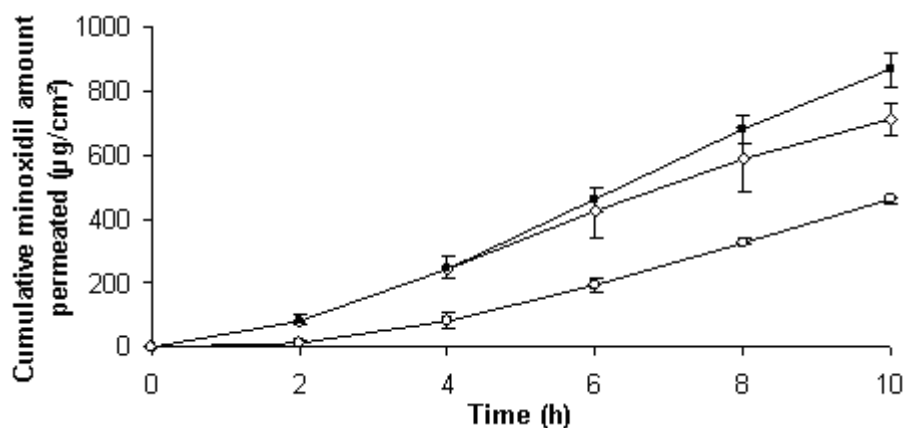


**Figure 5** Comparison of minoxidil permeation through porcine skin from different liposomal formulations (means  $\pm$  SD n=4): -■- EU coated liposomes; -◇- CS coated liposomes; -○- DPPC liposomes

The coating of liposomes with CS and EU improved the permeation of aciclovir 1.61-fold and 1.64-fold after 10 hours respectively, in comparison with control. In case of minoxidil the skin permeation was 1.54 times higher with CS and 1.88 with EU (Table 6). One of the reasons for this enhancement could be the negative charge on the epithelial cells surface, selective to positively charged liposomes [28]. Another reason of this effect might be the tendency of positive polymers to disrupt the tight junctions, which was confirmed in the case of CS [29]. Wydro et al showed also that CS significantly modifies lipids occurring in the skin [21].

**Table 6** Skin permeation rates of aciclovir and minoxidil from DPPC, CS DPPC and EU DPPC and influence of polymers on their permeation through porcine skin

Model drug	Formulation	Cumulative amount permeated after 10h ( $\mu\text{g}/\text{cm}^2$ )	Enhancement factor of polymers (CS and EU) compared to DPPC	Flux J ( $\mu\text{g}/\text{cm}^2/\text{h}$ )
Aciclovir	DPPC	744.61 $\pm$ 54.51	control	77.24 $\pm$ 5.5
	CS DPPC	1201.36 $\pm$ 203.6*	1.61	125.11 $\pm$ 19.5
	EU DPPC	1223.21 $\pm$ 131.9*	1.64	126.83 $\pm$ 13.9
Minoxidil	DPPC	460.56 $\pm$ 10.6	control	47.96 $\pm$ 5.9
	CS DPPC	713.18 $\pm$ 50.9*	1.54	79.64 $\pm$ 13.3
	EU DPPC	866.71 $\pm$ 52.6*	1.88	90.61 $\pm$ 5.9
Values are means $\pm$ SD n=4 *P<0.05 vs. DPPC (t-test)				

#### 4 Conclusion

It can be concluded that the physicochemical stability in terms of mean particle size and zeta potential of DPPC liposomes with and without aciclovir or minoxidil was significantly increased by addition of two different cationic polymers, CS and EU. According to microDSC data this phenomenon can be interpreted as hydrogen bonding between the polymer and liposome surfaces. Furthermore, FTIR spectra showed that aciclovir has strong hydrogen bonding with C=O groups of DPPC, whereas carbonyl groups were free in minoxidil presence. This data might be clarifying the longer stability of liposomes with minoxidil. The skin permeation efficiency of aciclovir and minoxidil from coated liposomes increased, what could be explained as a tendency of positively charged liposomes to interact stronger with the skin surface. Another possibility to explain this effect is that the CS and EU might be interacting with skin lipids and going deeper disrupting the tight junctions in lower epidermis layers.

## References

1. El Maghraby G.M. *et al.* Liposomes and skin: From drug delivery to model membranes. *Eur J Pharm Sci* 2008; 34: 203-222.
2. Biruss B., Valenta C., Skin permeation of different steroid hormones from polymeric coated liposomal formulations. *Eur J Pharm Biopharm* 2006; 62: 210-219.
3. Bouwstra J.A. *et al.* Structure of the skin barrier and its modulation by vesicular formulations. *Progress lipid res* 2003; 42: 1-36.
4. Cevc G., Vierl U. Nanotechnology and the transdermal route A state of the art review and critical appraisal. *J Control Release* 2010; 141: 277-299.
5. Mady M.M. *et al.* Biophysical studies on chitosan-coated liposomes. *Eur Biophys J* 2009; 381: 127-133.
6. Hasanovic A. *et al.* Chitosan-TPP nanoparticles as a possible skin drug delivery system for acyclovir with enhanced stability. *J Pharm Pharmacol* 2009; 61: 1609-1616.
7. Perugini P. *et al.* Study on glycolic acid delivery by liposomes and microspheres. *Int J Pharm* 2000; 196: 51-56.
8. Lopodota A. *et al.* The use of Eudragit RS 100/cyclodextrin nanoparticles for the transmucosal administration of glutathione. *Eur J Pharm Biopharm* 2009; 72: 509-520.
9. Alasino R.V. *et al.* Amphipathic and membrane-destabilizing properties of the cationic acrylate polymer Eudragit E100. *Macromol Biosci* 2005; 5: 207-213.
10. Quinteros D.A. *et al.* Interaction between a cationic polymethacrylate (Eudragit E100) and anionic drugs. *Eur J Pharm Sci* 2008; 33: 72-79.
11. Kählig H. *et al.* Chitosan-glycolic acid: a possible matrix for progesterone delivery into skin. *Drug Dev Ind Pharm* 2009; 1: 1-6.
12. Brandl M. *et al.* Liposome preparation by a new high pressure homogenizer Gaulin Micron Lab 40. *Drug Dev Ind Pharm* 1990; 16: 2167--2191.
13. Hasanovic A. *et al.* Analysis of skin penetration of phytosphingosine by fluorescence detection and influence of the thermotropic behaviour of



- DPPC liposomes. *Int J Pharm* 2010; 383: 14-17.
14. Skalko N. *et al.* Liposomes with nifedipin and nifedipin-cyclodextrin complex: calorimetric and plasma stability comparison. *Eur J Pharm Sci* 1996; 4: 359-366.
  15. Höller S., Valenta C. Effect of selected fluorinated drugs in a "ringing" gel on rheological behavior and skin permeation. *Eur J Pharm Biopharm* 2007; 66: 120-126
  16. Balakrishnan P. *et al.* Formulation and in-vitro assessment of minoxidil niosomes for enhanced skin delivery. *Int. J. Pharm.* 2009; 377: 1-8.
  17. Sinha V.R. *et al.* Stress studies on acyclovir. *J Chromatogr Sci* 2007; 45: 319-324.
  18. Laye C. *et al.* Formation of biopolymer-coated liposomes by electrostatic deposition of chitosan. *J Food Sci* 2008; 73: 7-15.
  19. Schneider T. *et al.* Surface modification of continuously extruded contrast-carrying liposomes: effect on their physical properties. *Int J Pharm* 1996; 132: 9-21.
  20. Kim D.H. *et al.* Fabrication and characterization of pseudo-ceramide-based liposomal membranes. *Colloids Surf B Biointerfaces* 2009; 73: 207-211.
  21. Wydro P. *et al.* Chitosan as a lipid binder: a langmuir monolayer study of chitosan-lipid interactions. *Biomacromolecules* 2007; 8: 2611--617.
  22. Auner B.G. *et al.* Interaction of phloretin and 6-ketocholestanol with DPPC-liposomes as phospholipid model membranes. *Int J Pharm* 2005; 294: 149-155.
  23. Wolka A.M. *et al.* The interaction of the penetration enhancer DDAIP with a phospholipid model membrane. *Int J Pharm* 2004; 271: 5-10.
  24. De Oliveira Tiera V.A. *et al.* Interaction of amphiphilic derivatives of chitosan with DPPC (1,2-dipalmitoyl-sn-glycero-3-phosphocholine). *J Therm Anal Calorim* 2009; 100: 309-313.
  25. Biruss B. *et al.* The influence of selected steroid hormones on the physicochemical behavior of DPPC liposomes. *Chem Phys Lipids* 2007; 148: 84-90.
  26. Severcan F. *et al.* Melatonin strongly interacts with zwitterionic model

- membranes--evidence from FTIR and differential scanning calorimetry. *Biochim Biophys Acta* 2005; 1668: 215-222.
27. Korkmaz F., Severcan F. Effect of progesterone on DPPC membrane: evidence for lateral phase separation and inverse action in lipid dynamics. *Arch Biochem Biophys* 2005; 440: 141-147.
  28. Yilmaz E., Borchert H.H., Design of a phytosphingosine-containing, positively-charged nanoemulsion as a colloidal carrier system for dermal application of ceramides. *Eur J Pharm Biopharm* 2005; 60: 91-98.
  29. Smith J. *et al.* Effect of chitosan on epithelial cell tight junctions. *Pharm Res* 2003; 21: 43-49.

#### **4.3 Modification of the conformational skin structure by treatment with liposomal formulation and its correlation to the penetration depth of aciclovir**

Amra Hasanovic<sup>1</sup>, Regina Winkler<sup>1</sup>, Günter Resch<sup>2</sup>, Claudia Valenta<sup>1</sup>

Submitted for publication November 2010

<sup>1</sup>University of Vienna, Department of Pharmaceutical Technology and Biopharmaceutics, Faculty of Life Sciences, Althanstrasse 14 1090 Vienna AUSTRIA

<sup>2</sup>IMP-IMBA-GMI Electron Microscopy Facility, Dr. Bohr-Gasse 3, 1030 Vienna, Austria

Corresponding Author: Claudia Valenta

Department of Pharmaceutical Technology and Biopharmaceutics

Faculty of Life Sciences

Althanstrasse 14

1090 Vienna

AUSTRIA

E-mail: [claudia.valenta@univie.ac.at](mailto:claudia.valenta@univie.ac.at)

Tel: +43 1 4277 55 410

Fax: +43 1 4277 9554

**Abstract**

The stratum corneum (SC), top layer of the epidermis, is comprised mostly of lipids, which are responsible for the permeability properties of the SC and which protect the body from external agents. Changes in these skin micro constituents can be understood by instrumental methods such as attenuated total reflectance Fourier transform infrared (ATR-FTIR) spectroscopy. The present work found that the types of skin analyzed, dermatomed abdominal porcine skin, pig ear skin and human heat separated skin, influenced both the shape and the intensity of recorded spectra. The typical FTIR spectral bands of the conformation of the lipid aliphatic chains in the skin samples were altered after treatment with pure DPPC liposomes and chitosan (CS) coated DPPC liposomes, but not with aqueous CS-solution. The conformational change could be the reason for the various permeability of skin. This was confirmed by tape stripping on pig ear skin (imitating in vivo studies): the amount of aciclovir penetrating from polymer coated and polymer free liposomes was significantly higher under the skin surface in comparison with the aqueous CS-solution. Moreover, the addition of the polymer to liposomes induced a higher skin penetration than pure liposomes. One explanation might be due to the CS's stronger adhesion to the skin.

**Keywords:** FTIR, Tape stripping, aciclovir, DPPC liposomes, cryo TEM

## 1 Introduction

The stratum corneum (SC) is a distinctive two compartment system, consisting of corneocytes embedded in the lipid matrix. The complex structure of the SC lipid bilayers is important in maintaining the barrier properties of skin [1, 2]. To understand the modification of the lipid organisation within the SC many techniques such as X-ray diffraction, IR spectroscopy, DSC,  $^2\text{H}$  NMR spectroscopy and electron microscopy are applied [3-5]. Most of the experimental evidences is consistent with the domain mosaic model suggested by Forslind et al., in which the skin lipids are organised in ordered domains (orthorhombic (OR) and hexagonal (HEX)) connected by lipids in a disordered phase (liquid-crystalline (LIQ)) [6-8]. It has been proposed that these domains would have crucial impact on SC permeability: the permeability of a disordered phase is in general greater than that of the ordered one [4]. According to Wertz et al. the greatest flux would be at the phase boundaries [6].

In the present study Fourier-transform infrared (FTIR) spectroscopy with attenuated total reflection (ATR) technique was performed. This is an optimal technique in determination of molecular vibration of the components in the SC at the functional group level [7]. The FTIR method has already been used to characterize the phase transitions of the SC lipids. These transitions were detected by shifting of methylen ( $\text{CH}_2$ ) bands of the lipid aliphatic chains [1, 2, 7, 9]. Therefore, in the first step the characteristic  $\text{CH}_2$  bands of dermatomed abdominal porcine skin, pig ear skin and human heat separated skin were compared and analyzed. In our last work ATR-FTIR method has been used to better understand interactions of the model drugs and two polymers with DPPC liposomes [10]. Based on these results, our intention was to further understand interactions between skin and different formulations. For this purpose the following formulations were applied: DPPC liposomes, chitosan (CS) coated DPPC liposomes as well as aqueous CS-solution. The liposomal formulations were additionally visualised by cryo-TEM. The question was whether the differences between polymer free and polymer containing liposomes could be seen. Because the previous studies showed higher aciclovir skin diffusion in vitro (Franz-cell model) from polymer coated versus polymer free liposomes additional penetration studies using the tape stripping method on pig ear skin

were performed [10]. With this method it is possible to investigate the drug distribution and penetration layer by layer of topical applied drugs in the SC [11-13].

## **2 Materials and methods**

### **2.1 Materials**

1,2-Dipalmitoyl-sn-glycero-3-phosphatidylcholine (DPPC) was purchased from Lipoid (Steinhausen, Switzerland). The product was synthetic Lipoid PC 16:0/16:0. The content of phosphatidylcholine was at least 99 % related to the dry weight. Chitosan (CS < 500 kDa) in the powder form was a gift from Syntapharm (Mülheim, Germany). The degree of deacetylation was determined by NMR with 95% [14]. Aciclovir was purchased from Fagron GmbH (Barsbüttel, Germany) All other chemicals used in this study were of analytical reagent grade and were used as received without any further purification.

### **2.2 Formulations**

Skin samples for FTIR experiments were treated with DPPC liposomes and chitosan (CS) coated DPPC liposomes, prepared as previously described [10]. Particle size was measured by a Zetasizer Nano ZS (Malvern Instruments, Malvern, United Kingdom). The 0.125% (w/w) aqueous CS-solution was produced by dissolving the polymer in 0.01M acetate buffer.

For the tape stripping procedure DPPC and CS coated liposomes were loaded with 1% aciclovir as reported [10]. Aciclovir, in aqueous CS-solution, was suspended in the same concentration.

#### **2.2.1 Encapsulation of aciclovir in liposomes**

Encapsulation of aciclovir in the liposomes was established by differential centrifugation method [15]. Briefly, liposomes and coated liposomes with aciclovir were centrifuged at 1200xg for 2 hours at 25°C (Hermle Z323K, Wehingen, Germany). The supernatants were removed and dissolved in 96% ethanol. Aciclovir content in the supernatants and in the precipitates was quantified by HPLC method specified previously (n=3) [10].

The encapsulation efficiency of aciclovir was calculated as described below:

$$\text{Encapsulation efficiency (EE\%)} = \frac{\text{Amount of bound drug}}{\text{Total amount of drug}} \times 100 = 24.38 \pm 0.40$$

## **2.3 Skin preparation for FTIR**

### **2.3.1 Abdominal porcine skin**

The full thickness abdominal skin without hair was dermatomed to a thickness of 1.2 mm and then stored frozen at -20°C. Skin samples with dimension of about 7.5 cm<sup>2</sup> (ZnSe crystal dimension) were adopted for the experiment, which was performed ten times.

The following treatments were applied:

- a) Application of 40 µl distilled water
- b) Application of 40 µl pure DPPC-liposomes
- c) Application of 40 µl coated CS-DPPC liposomes
- d) Application of 40 µl aqueous CS-solution
- e) Untreated skin (control)

After the treatment, the skin samples were placed in PBS buffer and kept at 37°C or 45°C in a closed petri dish for two hours in each case [4, 9].

### **2.3.2 Pig ear skin**

The same experimental procedure was repeated on pig ear skin prepared as described later (see 2.6.1.).

### **2.3.3 Human skin**

Human epidermis prepared by heat separation after plastic surgery underwent the same experimental procedure as porcine skin [16].

## **2.4 Attenuated total reflectance-Fourier transform infrared (ATR-FTIR)**

The penetration depth of IR is about 1 µm or less, which includes approximately 1–1.5 sheets of cell layers in the SC [9, 17]. Infrared spectra of the prepared skin samples were obtained by using FTIR spectrophotometer (model: Tensor 27, Bruker Optics, Ettlingen, Germany) with a photovoltaic MCT

detector at a temperature of 37°C (physiological temperature) and 45°C (transition temperature of SC lipids). To collect the spectra, the skin samples were placed stratum corneum down onto the ZnSe ATR crystal (tool: Bio-ATR I). To obtain the same intensity of spectra we put the cover glass on the sample. For data treatment we used the software OPUS 5.5.

## ***2.5 Cryo-Transmission electron microscopy (Cryo-TEM)***

Liposomes for cryo-TEM were frozen with a Leica EM GP immersion freezer (Leica Microsystems, Vienna, Austria) with its environmental chamber at 50 degC and 90% relative humidity. 4 µl of the specimen diluted to 2.5 mg/ml and pre-warmed to 50°C was applied onto glow discharged EM grid coated with perforated Quantifoil R3.5/1 carbon films (Quantifoil, Jena, Germany). After 30 s settling, the suspension was automatically blotted for 0.5-1.0 s with Whatman No. 1 filter paper and immediately plunged from the environmental chamber into liquid ethane. Subsequently, the specimens were handled only in the dehumidified working area and stored in liquid nitrogen prior to microscopy. The vitrified specimens were visualised on a Tecnai F30 'Helium' (Polara) cryo-TEM (FEI Company, Eindhoven, Netherlands) operated at 300 kV and cooled with liquid nitrogen. Micrographs were acquired at nominal magnification of 31 000x and at a defocus of -2.5 µm (high resolution, low contrast) and -8.0 µm respectively (high contrast, low resolution) and captured with a Gatan US4000 CCD camera.

## ***2.6 Tape stripping***

### ***2.6.1 Pig ear skin***

The pig ears were obtained from local butcher and stored in the refrigerator at -20°C. The night before the tape stripping procedure, the pig ears were stored in the fridge at 4°C. On the day of procedure the skin surface was cleaned with distilled water, dried and the hair were carefully removed by scissors as closely as possible to the surface.



### **2.6.2 Tape stripping**

The pig ears were fixed on a polystyrene support covered with aluminium foil, an area of 5X4 cm<sup>2</sup> was marked with a permanent marker and 5 µl/cm<sup>2</sup> of the tested formulation was applied. After one hour tape stripping was performed as described previously using Corneofix® tape strips [11, 18, 19]. Briefly, each tape strip was pressed on the skin with the roller over the paper for 5 seconds and then removed in a single quick movement. Every tape strip was placed onto the special slide frame to determine the mass of the removed SC. The pseudo-absorption of the skin corneocytes, which correlates with the protein amount on the removed tape strip, was established at 850 nm via infrared (IR) densitometer SquameScan<sup>TM</sup>850A (Heiland electronic, Wetzlar, Germany) as described previously [20, 21]. After the removal of 40 tape strips (the most of the SC) for all formulations, the model drug (aciclovir) was detectable up to the 10<sup>th</sup> strip. Therefore, only 10 strips were taken in all further experiments exhibited on 5 additional pig ears. To analyse aciclovir content in different layers of the skin, the tape strips (2x2 cm<sup>2</sup>) were extracted with 4 ml distilled water (1ml/cm<sup>2</sup>) respectively. The tubes were sonicated on ultra sonic bath for 12 min and afterwards centrifuged for 10 min. Aciclovir content was detected by HPLC using the method described previously [10].

### **2.6.3 Transepidermal water loss (TEWL) measurements**

The main aim of TEWL measurements was to characterise the barrier property of the pig ears. TEWL was recorded with closed chamber device (AquaFlux<sup>TM</sup>, Biox, London, UK) before and after the tape stripping procedure. Measurements were performed in triplicate and AquaFlux<sup>®</sup> V6.2 software was used for data analysis.

### **2.7 Statistics**

Results of all studies are presented as the means of at least three experiments ± SD. Data were exported to the GraphPad Prism statistics software package (GraphPad Prism Software, USA). Analysis groups consisted of independent mean values and the Gaussian distribution of the data was verified using the Kolmogorov-Smirnov test. A statistical analysis was performed using one-way

ANOVA with post-hoc Dunnet's or Tukey's test. P-values of  $< 0.05$  were considered significant.

### 3 Results and discussion

ATR-FTIR spectroscopy is a non-invasive technique for characterisation of the SC at a molecular level. Different attempts have been made to present IR spectra of skin [2, 3, 9]. In the present study IR spectra of dermatomed abdominal porcine skin, pig ear skin and human heat separated skin are compared (Fig.1). The following skin bands obtained from skin intercellular lipids and keratin (corneocytes) were of interest:  $\text{CH}_2$  asymmetric ( $\sim 2920 \text{ cm}^{-1}$ ) and symmetric stretching vibration ( $\sim 2850 \text{ cm}^{-1}$ ),  $\text{CH}_2$  scissoring mode between  $1470$  and  $1460 \text{ cm}^{-1}$ , amid I ( $\text{C}=\text{O}$ ) vibration at about  $1640 \text{ cm}^{-1}$  and amid II ( $\text{C}-\text{N}$ ) vibration at about  $1540 \text{ cm}^{-1}$  as well as  $\text{C}=\text{O}$  stretching band from the fatty acids at about  $1740 \text{ cm}^{-1}$  [7, 9]. In Fig. 1 it can be clearly seen that the human heat separated skin shows similar spectra to the dermatomed abdominal porcine skin as well as to the pig ear skin.

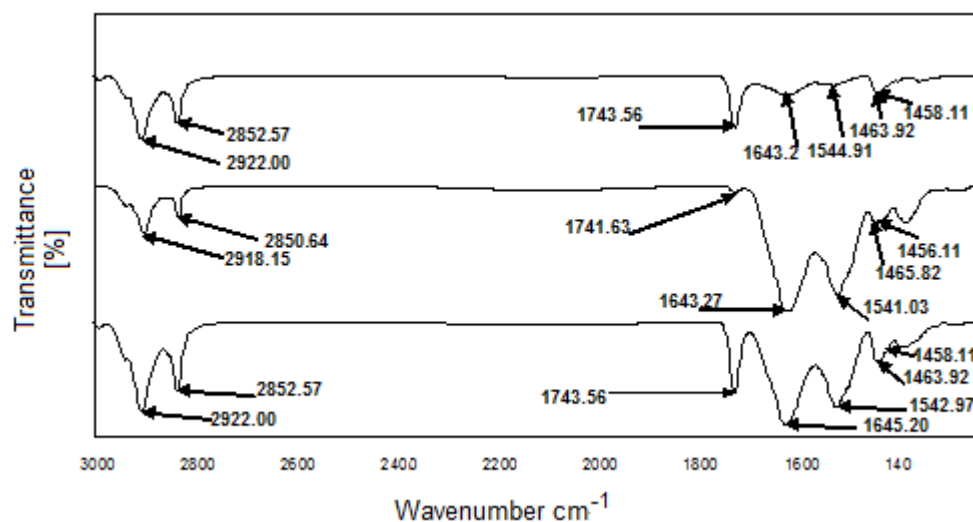


**Figure 1** Comparison of FTIR transmission spectra at  $37^\circ\text{C}$  of untreated pig abdominal dermatomed, pig ear and human skin (from top to bottom)

These different skins have been employed for studying the influence of different formulation treatments on the characteristic vibration of the IR-spectra. For this purpose preliminary experiments were necessary. The amount of formulation applied, number of treatments and time of impregnation were optimised. The amount of 40  $\mu$ l formulation to be used was established according to the length of time taken to be absorbed by the skin. This was in agreement with already published data [4, 9]. Procedures using repeated applications and longer impregnation periods have not shown any significant differences in the obtained spectra (data not shown). According to the investigations undertaken, an application of 40  $\mu$ l formulation impregnated with skin for 2 h was found to be optimal for spectra interpretation. In Tables 1 and 2 the band wavenumbers of different skin spectra (37°C and 45°C) impregnated with pure DPPC, CS coated liposomes as well as with the aqueous CS-solution and distilled water respectively, are presented. The control modes (untreated skin) in all spectral regions, except the C=O region of pig ear skin and human skin, remained unaltered by an increase of temperature from 37° to 45°C. This contrasts with data published by other authors that did show change across this temperature range [4, 9, 22].

Of particular interest for studying the interaction of the formulations with SC lipids are CH<sub>2</sub> stretching bands. Analyses of these bands provide information about conformational order (trans-gauche isomerisation) of the lipid alkyl chains [4, 23, 24]. After the treatment dermatomed porcine skin and human skin with liposomal formulations, symmetric and asymmetric methylene stretching bands were shifted to significantly lower values compared with the control samples, indicating a lipid order-disorder transition from the gel to the liquid-crystalline state (Table 1 and 2). This transition involves also an increase in the fluidity of the SC lipids that could increase the skin penetration [4]. However, the same treatments of pig ear skin showed the shift of symmetric stretching band to the lower values only at 45°C.

The region corresponding to CH<sub>2</sub> scissoring vibration provides information about the lateral packing of lipid alkyl chains in the SC. In all skin samples at both temperatures (37° and 45°C) CH<sub>2</sub> scissoring band displayed a doublet, characteristic of the orthorhombic (OR) lattice, which is very important for the

barrier function of the lipids (Table 1 and 2) [9, 25]. This doublet is caused by short-range interaction between the CH<sub>2</sub> in the lipid tails [22]. The split of the band is indicative of the degree of inter-chain interaction and the size of the domain with OR organisation. In the spectra of the pig ear skin the scissoring width was ~10 cm<sup>-1</sup> indicating a high content of OR phase. The corresponding value observed in dermatomed porcine skin and human skin was ~ 6 cm<sup>-1</sup> displaying lower content of OR phase and higher conformational disorder of the lipid chains than in pig ear skin [2]. The treatment with liposomal formulations showed slight increase of width of the doublet at both temperatures (Table 1 and 2). In conclusion, the FTIR data suggest that the SC barrier function is partially overcome by liposomal application.

**Table 1** ATR-FTIR values of characteristic bands of different skin modes at 37°C

	Dermatomed porcine skin modes (cm <sup>-1</sup> )				Pig ear skin modes (cm <sup>-1</sup> )				Human skin modes (cm <sup>-1</sup> )			
	CH <sub>2</sub> sym.str etching	CH <sub>2</sub> asym. stretchi	C=O	CH <sub>2</sub> scissori ng	CH <sub>2</sub> sym.str etching	CH <sub>2</sub> asym.s tretchin	C=O	CH <sub>2</sub> scissori ng	CH <sub>2</sub> sym.str etching	CH <sub>2</sub> asym.s tretchin	C=O	CH <sub>2</sub> scissori ng
Control	2922.0	2852.5	1743.5	1458.1 1463.9	2918.1	2850.6	1741.6	1456.1 1465.8	2922.0	2852.5	1743.5	1458.1 1463.9
Water	2922.0	2852.5	1743.5	1458.1 1463.9	2918.1	2850.6	1741.4	1456.1 1465.8	2922.0	2852.5	1743.5	1458.1 1463.9
DPPC	2918.1 <sup>a</sup>	2850.6 <sup>a</sup>	1742.2 <sup>a</sup>	1456.1 1467.1	2918.1	2850.6	1738.4 <sup>a</sup>	1456.1 1467.7	2920.0 <sup>a</sup>	2850.6 <sup>a</sup>	1743.5	1458.1 1465.8
CS- DPPC	2918.7 <sup>a</sup>	2850.6 <sup>a</sup>	1741.6 <sup>a</sup>	1456.1 1465.8	2918.1	2850.6	1738.4 <sup>a</sup>	1456.1 1467.7	2920.0 <sup>a</sup>	2850.6 <sup>a</sup>	1743.5	1458.1 1465.8
CS- solutio	2922.0	2852.5	1743.5	1458.1 1463.9	2918.1	2850.6	1741.2	1456.1 1465.8	2921.3	2852.5	1743.5	1458.1 1463.9

Values are means of n=10

<sup>a</sup>Significantly decreased values compared with the control (Dunnet's test)

**Table 2** ATR-FTIR values of characteristic bands of different skin modes at 45°C

	Dermatomed porcine skin modes (cm <sup>-1</sup> )				Pig ear skin modes (cm <sup>-1</sup> )				Human skin modes (cm <sup>-1</sup> )			
	CH <sub>2</sub> sym.str etching	CH <sub>2</sub> asym. stretchi	C=O	CH <sub>2</sub> scissori ng	CH <sub>2</sub> sym.str etching	CH <sub>2</sub> asym.s tretchin	C=O	CH <sub>2</sub> scissori ng	CH <sub>2</sub> sym.str etching	CH <sub>2</sub> asym.s tretchin	C=O	CH <sub>2</sub> scissori ng
Control	2922.0	2852.5	1743.5	1458.1 1463.9	2918.1	2850.6	1743.5	1456.1 1465.8	2922.0	2852.5	1745.1	1458.1 1463.9
Water	2922.0	2852.5	1743.5	1458.1 1463.9	2918.1	2850.6	1743.5	1456.1 1465.8	2922.0	2852.5	1745.1	1458.1 1463.9
DPPC	2919.4 <sup>a</sup>	2850.6 <sup>a</sup>	1742.2 <sup>a</sup>	1458.1 1465.8	2916.1 <sup>a</sup>	2850.6	1738.4 <sup>a</sup>	1456.1 1467.7	2918.7 <sup>a</sup>	2850.6 <sup>a</sup>	1742.9 <sup>a</sup>	1456.1 1465.8
CS- DPPC	2918.7 <sup>a</sup>	2850.6 <sup>a</sup>	1741.6 <sup>a</sup>	1458.1 1465.8	2916.8 <sup>a</sup>	2849.3	1737.1 <sup>a</sup>	1456.1 1467.7	2918.1 <sup>a</sup>	2850.6 <sup>a</sup>	1742.9 <sup>a</sup>	1456.1 1465.8
CS- solutio	2922.0	2852.5	1743.5	1456.1 1463.9	2918.1	2850.6	1741.2 <sup>a</sup>	1456.1 1465.8	2921.3 <sup>a</sup>	2852.5	1745.4 <sup>a</sup>	1458.1 1463.9

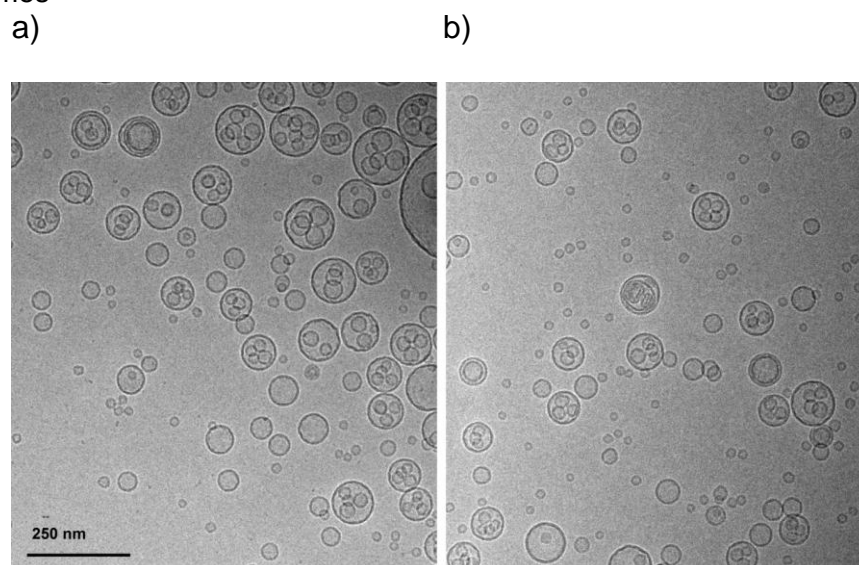
Values are means of n=10

<sup>a</sup>Significantly decreased values compared with the control (Dunnet's test)

In order to obtain more insight into structure of the liposomes cryo-TEM was applied. As seen in Fig. 2 there were mainly multivesiculare liposomes [26]. The difference in liposomes induced by polymers could not be visualised by this technique. However, comparing Fig. 2a and Fig. 2b, CS containing liposomes seem to be more distant from each other. This could be explained by the positive charge of CS, which decreased the tendency of liposome-aggregation, resulting in their longer stability.

Furthermore, tape stripping was performed on pig ears to establish the penetration depth of the model drug (aciclovir) from the formulations mentioned above (pure DPPC, CS coated liposomes and aqueous CS-solution). According to Herkenne et al. and Lindemann et al. data obtained in ex vivo on pig ear are comparable to those observed in vivo in humans [27, 28]. The most SC has been removed after approximately 40 strips confirmed by TEWL values of 80 gm<sup>-2</sup>h<sup>-1</sup> [29].

**Figure 2** Cryo-TEM micrographs of a) pure DPPC liposomes and b) CS coated DPPC liposomes



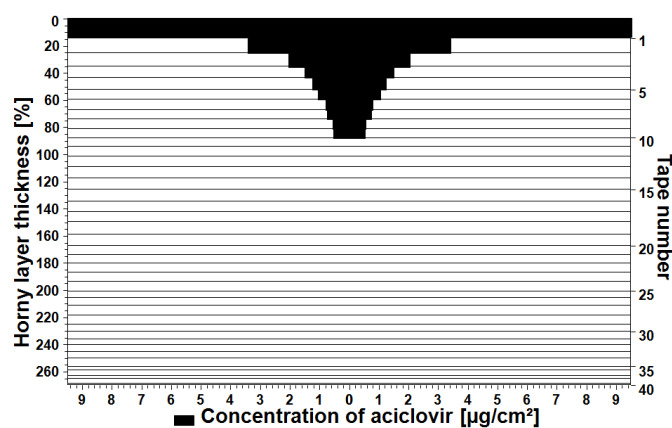
The maximal penetration depth of aciclovir was detectable until the 10<sup>th</sup> strip from all three tested formulations (Fig. 3abc.). The TEWL values measured before and after the tape stripping were increased from about 14 to 30 gm<sup>-2</sup>h<sup>-1</sup>. This is in accordance with findings of electron microscopy studies on humans, where liposomes did not penetrate deeper than the horny layer [30]. The findings of presents work are also in agreement with other studies, where particles greater than 10 nm (we produced liposomes of ~90nm) did not penetrate the SC [31, 32]. The concentration of aciclovir in SC was related to the amount of corneocytes on each tape strip analysed by IR densitometer [20]. As seen in Table 3 the formulations applied did not significantly influence the amount of removed corneocytes in the first strip in comparison with untreated skin. Also the difference between the formulations considering the amount of removed corneocytes was not evident (Fig. 3abc.). Aciclovir from the aqueous CS-solution was detected in significantly higher amount on the skin surface, which was presented by the first tape strip, than from liposomal formulations (Table 3) indicating the better aciclovir penetration from liposomes. This was expected since liposomes have been claimed to improve drug deposition within the SC [33]. As seen also in Table 3, CS coated liposomes induced significantly improved aciclovir penetration into the SC compared to pure liposomes. This was in agreement with our previously published data: aciclovir penetrated

greater from CS coated liposomes than from CS free liposomes [10]. One of the reasons might be the positive charge of CS, leading to tight SC adhesion.

a)



b)



c)

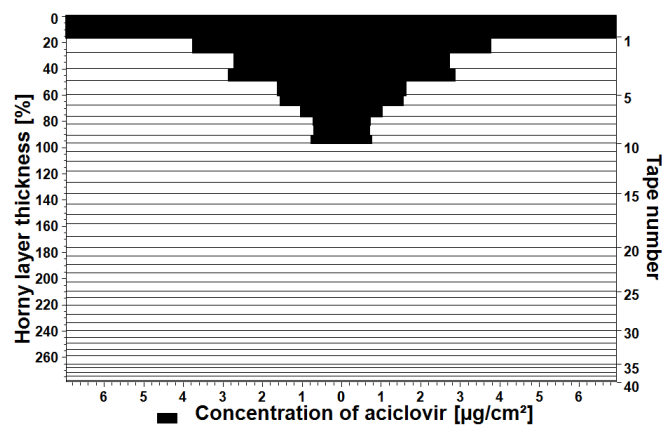


**Figure 3** Penetration profile of the aciclovir containing formulations: a) aqueous CS-solution, b) DPPC liposomes and c) CS coated liposomes

**Table 3** Aciclovir concentration in the first tape strip of the removed stratum corneum

	Untreated skin	Skin treated with CS-DPPC	Skin treated with DPPC	Skin treated with CS-solution
Corneocytes (%)	19.80 ± 4.66 <sup>a</sup>	21.02 ± 0.96 <sup>a</sup>	18.77 ± 1.45 <sup>a</sup>	24.32 ± 1.55 <sup>a</sup>
Aciclovir (µg/cm <sup>2</sup> )	-	13.89 ± 2.79 <sup>b</sup>	18.99 ± 2.51 <sup>b</sup>	25.26 ± 2.85 <sup>b</sup>

Values are means ± SD of six experiments.  
<sup>a</sup> P > 0.05 (Tukey's test)  
<sup>b</sup> P < 0.05 (Tukey's test)

#### 4 Conclusion

The FTIR results of this work appear to confirm the physiological similarities between pig skin and human skin: pig skin makes a good skin model for FTIR studies. Dermatomed abdominal porcine skin was especially suitable for this experiment due to its simple preparation. The skin treatments with liposomal formulations resulted in a partially decreased orthorhombic organisation or reduced barrier function. These data were confirmed by penetration studies. Using the tape stripping method the higher aciclovir penetration from CS coated liposomes versus polymer free liposomes was observed, verifying our previously published studies.

#### Acknowledgements

We would like to thank Prof. Dr. Jürgen Lademann, Dr. Hans-Jürgen Weigmann and Mrs. Sabine Schanzer, Department of Dermatology, University Hospital Charité, for tape stripping coaching and data presentation support.



## References

1. Lafleur M. Phase behaviour of model stratum corneum lipid mixtures: an infrared spectroscopy investigation. *Can J Chem* 1998; 76: 1501-1511.
2. Boncheva M. *et al.* Molecular organisation of the lipid matrix in intact stratum corneum using ATR-FTIR spectroscopy. *Biochim Biophys Acta* 2008; 1778: 1344-1355.
3. Moore D., Rerek M.E. Insight into the molecular organisation of lipids in the skin barrier from IR spectroscopy studies of stratum corneum lipids. *Acta Derm Venereol* 2000; Supp 208: 16-22.
4. Rodríguez G. *et al.* Conformational changes in SC lipids by effect of bicellar systems. *Langmuir* 2009 18: 10595-10603.
5. Bouwstra J.A. *et al.* Structural investigations of human stratum corneum by small-angle x-ray scattering. *J Invest Dermatol* 1991; 97: 1005-1012.
6. Wertz P.W. Lipid and barrier function of the skin. *Acta Derm Venereol* 2000; Supp 208: 7-11.
7. Obata Y. *et al.* Infrared spectroscopic study of lipid interaction in stratum corneum treated with transdermal absorption enhancers. *Int J Pharm* 2010; 389: 8-23.
8. Forslind B. *et al.* A novel approach to the understanding of human skin barrier function. *J Dermatol Sci* 1997; 14: 115-125.
9. Rodríguez G. *et al.* Application of bicellar systems on skin: diffusion and molecular organization effects. *Langmuir* 2010; 26: 10578-10584.
10. Hasanovic A. *et al.* Improvement in physicochemical parameters of DPPC liposomes and increase in skin permeation of aciclovir and minoxidil by the addition of cationic polymers. *Eur J Pharm Biopharm* 2010; 72: 148-153.
11. Weigmann H.J. *et al.* Comparison of human and porcine skin for characterization of sunscreens. *J Biomed Opt* 2009; 14: 1-6.
12. Escobar-Chavez J.J. *et al.* The tape-stripping technique as a method for drug quantification in skin. *J Pharm Pharmaceut Sci* 2008; 11: 104-130.
13. Jacobi U. Estimation of the relative stratum corneum amount removed by tape stripping. *Skin Res Technol* 2005; 11: 91-96.

14. Kählig H. *et al.* Chitosan-glycolic acid: a possible matrix for progesterone delivery into skin. *Drug Dev Ind Pharm* 2009; 1: 1-6.
15. Montenegro L. *et al.* Quantitative determination of hydrophobic compound entrapment in dipalmitoylphosphatidylcholine liposomes by differential scanning calorimetry. *Int J Pharm* 1996; 138: 191-197.
16. Valenta C. Effect of phloretin on the percutaneous absorption of lignocaine across human skin. *J Pharm Sci* 2001; 90: 485-492.
17. Sakuyama S. *et al.* Analysis of human face skin surface molecules in situ by Fourier-transform infrared spectroscopy. *Skin Res Technol* 2010; 16: 151-160.
18. Teichmann A. *et al.* Comparison of stratum corneum penetration and localization of a lipophilic model drug applied in an o/w microemulsion and an amphiphilic cream. *Eur J Pharm Biopharm* 2007; 67: 699-706.
19. Löffler H. *et al.* Stratum corneum adhesive tape stripping: influence of anatomical site, application pressure, duration and removal. *Br J Dermatol* 2004; 151: 746-752.
20. Voegeli R. *et al.* Efficient and simple quantification of stratum corneum proteins on tape strippings by infrared densitometry. *Skin Res Technol* 2007; 13: 242-251.
21. Hahn T. *et al.* Infrared densitometry: a fast and non-destructive method for exact stratum corneum depth calculation for in vitro tape-stripping. *Skin Pharmacol Physiol* 2010; 23: 183-192.
22. Caussin J. *et al.* Lipid organisation in human and porcine stratum corneum differs widely, while lipid mixture with porcine ceramides model human stratum corneum lipid organisation very closely. *Biochim Biophys Acta* 2008; 1778: 1472-1482.
23. Pensack R.D. *et al.* Infrared kinetic/structural studies of barrier reformation in intact stratum corneum following thermal perturbation. *Appl Spectrosc* 2006; 60: 1399-1404.
24. Prasch T.H. *et al.* Infrared spectroscopy of the skin: influencing the stratum corneum with cosmetic products. *Int J Cosmet Sci* 2000; 22: 371-373.
25. Caussin J. *et al.* Hydrophilic and lipophilic moisturizers have similar

- penetration profiles but different effects on SC water distribution in vivo, *Experiment Dermatol* 2009; 18: 954-961.
26. Müller R.H., Hildebrand G.E., Pharmazeutische Technologie: Moderne Arzneistoffe, Wissenschaftliche Verlagsgesellschaft mbH, Stuttgart, Germany, 1998, pp. 219-222
  27. Herkenne C. *et al.* Pig ear skin ex vivo as a model for in vivo dermatopharmacokinetic studies in man. *Pharm Res* 2006; 23: 1850-1856.
  28. Lindemann U. *et al.* Quantification of the horny layer using tape stripping and microscopic techniques. *J Biomed Opt* 2003; 8: 601-607.
  29. Wu X. *et al.* Drug delivery to the skin from sub-micron particles formulations: Influence of particle size and polymer hydrophobicity. *Pharm Res* 2009; 26: 1995-2001.
  30. Korting H.C., Schaller M. Interaction of liposomes with human skin: the role of the stratum corneum. *Adv Drug Delivery Rev* 1996; 18: 303-309.
  31. Baroli B. *et al.* Penetration of metallic nanoparticles in human full-thickness skin. *J Invest Dermatol* 2007; 127: 1701-1712.
  32. Sonavane G. *et al.* In vitro permeation of gold nanoparticles through rat skin and rat intestine: Effect of particle size. *Coll Surf B: Biointerface* 2008; 65: 1-10.
  33. El Maghraby G.M. *et al.* Liposomes and skin: From drug delivery to model membranes. *Eur J Pharm Sci* 2008; 34: 203-222.

#### **4.4 Analysis of skin penetration of phytosphingosine by fluorescence detection and influence of the thermotropic behaviour of DPPC liposomes**

Amra Hasanovic<sup>1</sup>, Sonja Hoeller<sup>1</sup>, Claudia Valenta<sup>1</sup>

Int. J. Pharm. 2010, 383: 14-17

<sup>1</sup>University of Vienna, Department of Pharmaceutical Technology and Biopharmaceutics, Center of Pharmacy, Faculty of Life Sciences

Althanstrasse 14

1090 Vienna

AUSTRIA

Claudia Valenta

E-mail: [claudia.valenta@univie.ac.at](mailto:claudia.valenta@univie.ac.at)

Tel: +43 1 4277 55 410

Fax: +43 1 4277 955

**Abstract**

Phytosphingosine (PS) is a promising compound in skin formulations, considering its application in the treatment of acne and different inflammations as well as in the 'anti age' cosmetics. PS, as an active substance was incorporated in DPPC liposomes intended to standard diffusion experiments, where dermatomed porcine skin was mounted in FRANZ-cells. The proved skin retention was about 5.5% (w/w) after 24 hours and about 6.8% (w/w) after 48 hours of the applied PS amount, whereas only about 0.05% (w/w) and about 0.07% (w/w) PS, respectively, could be observed in the acceptor medium. To increase analytical sensitivity PS was derivatised by o-phthalaldehyde (OPA) reagent and analysed by HPLC with fluorescence detection. The higher amount of PS within the skin symbolised an interaction with lipid structures in skin. Further evaluation of this interaction was accomplished by applying microDSC studies of PS with DPPC as a model membrane. For this purpose liposomes were prepared by increasing PS content. The characteristic endothermic peak observed for the single system was shifted to a slightly higher temperature and broadened as the mole fraction of PS increased. This might be the effect of mixing of PS with DPPC. An addition of 10 mol% PS resulted in more than double sized particles pointing to a possible change in the liposomal shape.

**Keywords:** DPPC-liposomes, phytosphingosine, DSC, OPA-reagent

## 1 Introduction

The free sphingoid base phytosphingosine (PS) is naturally found in cell membranes of a human body and is present in small amounts in the epidermis [1]. PS is involved in keratinocytes differentiation and anti-inflammation [2]. In several studies PS showed anti-microbial properties against probionibacterium acnes and staphylococcus aureus and therefore effectively reduced signs of acne. Furthermore, there are investigations confirming that PS reduced redness of inflamed skin [3, 4]. Its positive influence on the skin permeation of fludrocortisone acetate and flumethasone pivalate in nanoemulsions formulations was documented by our group [5]. Recently an additionally preventive effect of PS on UV-induced decrease of pro-collagen was demonstrated in human dermal fibroblasts. Moreover, PS showed the inhibition of UV-induced IL-6 and COX2 gene expression. These results indicate that topically applied PS has anti-aging properties pointing to the potential use of PS as a therapeutic agent in the prevention and treatment of extrinsic aging [6]. Due to all these studies, PS could be considered as an ideal active ingredient for different pharmaceutical and cosmetic applications whose biological activity can be enhanced by the use of an appropriate formulation. DPPC liposomes, spherical bilayer vehicles, have been chosen due to ability to encapsulate oil soluble components, increase their stability and maintain their activity in different environments [7]. Moreover, they are able to increase concentration of the compound in the epidermis and in the deeper layers of the skin probably through the similarity of their lipid bilayer to that in the skin [8].

In the first part the PS amount of skin penetration as well as skin retention from DPPC liposomes were investigated. For this purpose we performed diffusion studies on dermatomed porcine skin placed in FRANZ cells. The analytical method following derivatisation of PS involving HPLC was successful. It was simple, sensitive and exact, due to fluorescence detection.

In the second part DPPC liposomes were used as model membranes to gain more information about their interaction with PS. MicroDSC studies investigating the influence of PS on DPPC thermotropic behaviour were selected.

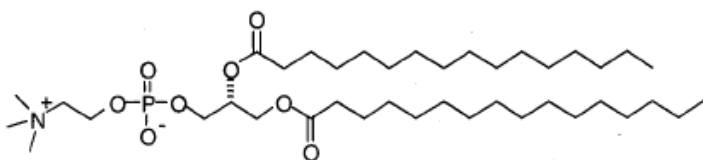
## 2 Materials and Methods

### 2.1 Materials

1,2-Dipalmitoyl-sn-glycero-3-phosphatidylcholine (DPPC) was purchased from Lipoid (Switzerland). The product was Lipoid PC 16:0/16:0. According to its specification the content of phosphatidylcholine related to the dry weight was at least 99 %. Phytosphingosine was kindly provided by Degussa (Cosmoferm BV, NL). All other chemicals used in this study were of analytical reagent grade and were used as received without any further purification.

The chemical structures of DPPC and PS are presented in Figure 1.

a



b

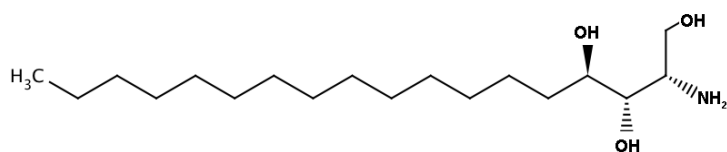


**Figure 1** (a) Chemical structure of DPPC and (b) chemical structure of PS

### 2.2 Preparation of Liposomes

DPPC liposomes were prepared according to a modified method of Thompson et al. [1]. Briefly, the phospholipid powder was dispersed in distilled water at 60°C in an end concentration of 2.5% (w/w) and magnetically stirred until the powder was completely dissolved and thoroughly mixed using an ultra-Turrax (Omni 500). Afterwards the dispersion was homogenised with a high-pressure homogeniser (EmulsiFlex-C3, Avestin) for sixteen times at approximately 1100 bar. The liposomes were kept at 4 °C over night and characterised the day after in terms of mean particles size and PDI. Into these liposomes PS was incorporated directly in the following concentration: 2.5, 5 and 10 mol%,

respectively, and mechanically stirred for 24 hours at 60°C. The resulting liposomes were used for microDSC studies. For the diffusion experiments, liposomes loaded with 0.2% (w/w) PS were prepared in the same conditions.

### **2.3 Diffusion studies**

In vitro permeation studies with porcine abdominal skin were performed as previously reported [9]. To obtain optimal sink conditions the receptor compartment was filled with 2 ml of 0.02 M phosphate buffer adjusted with lactic acid to pH 5. Since the concentration of PS actually used in cosmetics is 0.05-0.2% (w/w), about 0.5-0.7 ml of 0.2% (w/w) PS-loaded liposomes were applied to the skin surface. Application of the liposomes was defined as the starting point of the procedure. Two independent sets of experiment were performed: one for 24 and one set for 48 hours. Samples were drawn, centrifuged at 17 586×g for 6 minutes. Subsequently the supernatants were discarded and frozen at -20 °C. They were then freeze-dried under the following conditions: at -30 °C for 3 hours and afterwards at -55 °C over night. The lyophilisates were resuspended in ethanol. Each batch was derivatized with OPA-reagent prior to quantification by HPLC.

Additionally experiments were performed in order to analyse the content of the permeated PS in the skin 24 and 48 hours after application, respectively. At the end of each experiment sample-applied skin was wiped with paper than sliced and homogenised with a defined amount of ethanol, vortexed for 30 s and stirred over night. After centrifugation, supernatants were derivatized with OPA-reagent and quantified by HPLC as described in 2.4. Due to the naturally occurring PS in the epidermis we additionally carried out parallel experiments with PS-free liposomes. The measured PS concentration in the skin was about 0.1 µg±0.03 per cm<sup>2</sup> and therefore negligible.

### **2.4 OPA-reagent derivatization and HPLC analyses**

The OPA-reagent derivatization was accomplished as previously described by Min et al. [10]. Briefly, the sample solution was mixed with OPA reagent (5 mg o-phthalaldehyde, 25 µl 2-mercaptoethanol, 0.5 ml ethanol and 50 ml borate buffer pH 10.5) in 1:1 ratio for 2 min and incubated at room temperature for 30



min. The eppendorf tube was light protected to prevent degradation of OPA reagent [10].

The HPLC analysis was performed using C-18 RP column (Nucleosil 100-5, 250 mm x 4 mm, Macherey-Nagel, Germany) at 1 ml/min flow rate, with acetonitrile/water 90/10. The fluorescence intensity of the eluate was monitored at a wavelength of 370/460 nm excitation/emission by fluorescence detector (LS40, Perkin Elmer). Ethanol standard solutions of PS in the range from 0.3 to 100 µg/ml (n=7) were derivatised with OPA-reagent and used to construct the calibration curve. Linearity was determined by the elaboration of three standard calibration curve (every fresh prepared). A very high correlation of  $0.9998 \pm 0.0002$  was obtained. The deviations of all points of calibration curve of PS were in the range of 1.1 to 2.5% of the slope of the corresponding regression equation.

### **2.5 Particle size measurement of liposomes**

The mean particle size and size distribution were determined by photon correlation spectroscopy with a Zetasizer Nano ZS (Malvern, UK) at 25°C. The liposomes dispersion was diluted to the appropriate concentration with deionised water after 24 hours of preparation. The size distribution was represented by the polydispersity index (PDI) values. The measurements were performed using a He-Ne laser at 633nm.

### **2.6 Micro-Differential scanning calorimetry (microDSC) studies**

Differential thermal analysis was performed using a Setaram III micro-calorimeter. Samples of pure and PS loaded liposomes, prepared as described in 2.2 were scanned. The measurements conditions were: 1°C/min for the scanning rate over the temperature range 15-65°C, using purified water as reference. Thermal transitions were calculated using Setsoft 2000 Setaram software. After baseline subtraction, raw power data were converted to molar heat capacity data. Baselines were fitted to the pre-transition and main transition regions using a linear baseline function so that transition temperatures and enthalpies of reaction could be calculated for each lipid concentration

## **2.7 Statistical data analyses**

Results of all studies are expressed as the means of at least three experiments  $\pm$  SD. Statistical data analysis was performed using t-test with  $P < 0.05$  as minimal level of significance.

## **3 Results and Discussion**

Due to increasing number of atopic eczema and pruritic diseases, new dermal preparations with the anti-inflammatory PS are of a great interest. Recently, additional penetration enhancing effect on the skin permeation of fludrocortison acetate and flumethasone pivalate was shown [5]. Therefore, PS could have the extra benefit of reducing topical corticosteroids acting as a multifunctional drug.

In a first part of our research the amount of penetrated PS through porcine skin was measured. Due to the high lipophilicity of the PS (LogP 5.18), it could be expected that its main amount would be restored within the skin. In pre-liminary experiments it was seen that an HPLC analytic of PS with UV detection could not be used due to the very small PS amount remained under the detection limit. Therefore a more sensitive method using fluorescence detection was achieved. To gain a fluorescent detectability PS was labelled by o-phthalaldehyde (OPA) reagent. Previously this method was useful for measurement of different sphingoid bases in biological samples [10]. The derivatisation relied on chemical reaction between o-phthalaldehyde and the primer amine group of PS in presence of reduced sulphur compound mercaptane. The obtained product, iso-indole, was analysed by HPLC using fluorescence detection. Diffusion experiments were run for 24 and 48 hours, respectively, after which the skin was shredded and analysed for PS. The applied amount of liposomes corresponded to an infinite dose. As seen in Table 1 after 24 hours about 5.5% (w/w) and after 48 hours about 6.8% (w/w) of the applied PS amount was retained within the skin whereas only a small PS concentration of about 0.05 % (w/w) and about 0.07% (w/w) could be detected in the receiver compartment after 24 and 48 hours of diffusion, respectively. Interestingly no significant increase of PS in the acceptor medium can be achieved after 48 hours compared to 24 hours of diffusion. This result may

indicate an interaction of PS with structures within the skin.

**Table 1** Skin retention, cumulative permeated amount and amount in the donor compartment of PS in % of the applied amount after 24 hours (one set of experiments, and after 48 hours (one set of experiments) of diffusion

Time (hours)	PS (donor) (%)	PS (retained) (%)	PS permeated amount (%)
24	94 ± 9	5.5 ± 2.4	0.05 ± 0.002
48	93 ± 16	6.8 ± 0.8	0.07 ± 0.002

Values are means ± SD n=3

In order to obtain a better understanding of the mechanism of this interaction of PS, microDSC studies with DPPC as a model membrane were performed [11, 12]. Although we are aware that the lipid composition of skin is completely different, DPPC liposomes, due to their, simplicity, were used as a model membrane for many other studies [13-15].

Since DPPC is a widely used model for lipid bilayers and its transition temperature  $T_{max}$  can be easily measured as it has a narrow main endothermic peak at 41.4 °C (gel-to-liquid crystalline phase  $P\beta' \rightarrow L\alpha$ ), where the lipid acyl chains in an all-trans configuration undergoing a chain melting transition at a temperature,  $T_{max}$ , to liquid crystalline phase with the chains having both trans as well as gauche configurations [11, 15, 16]. A smaller pre-transition, which appears near 34.4°C reflecting the lamellar gel to rippled gel ( $L\beta' \rightarrow P\beta'$ ) transition in the gel phase [11, 13, 15-17] The pre-transition has been generally attributed on the surface structure of the vehicle and is related to rotations of the phospholipid head groups or transformation in the lamellar structure and changes in the hydrocarbon chain packing [13]. Figure 2 gives the microDSC curves of the DPPC-PS loaded liposomes. As seen in Table 2, the characteristic endothermic peak observed for the single system is shifted to a slightly higher temperature and broadened as the mole fraction of PS increased. This effect on main transition endotherm may be explained as a result of mixing of PS with DPPC. This is in agreement with other studies investigating the similar structured stearylamine interacting with DPPC [18]. In other words, the higher transition temperature observed from the compositions of DPPC and PS may indicate closer packing of the DPPC and PS molecules

forming the lamellar bilayers. On the one hand the preferential partition of the lipophilic compound, PS, into the lipid domains of the bilayer structure by incorporation is expected. On the other hand the disappearance of the pre-transition (Table 2) indicates an interaction with the polar region as well [13, 15]. Moreover, an incorporation of 10 mol% PS was able to increase the liposome size more than twice (Table 3). This might be explained as a change of the shape of multilamellar vesicles (MLV) to large unilamellar vesicles (LUV) and due to the charge effect of PS [5, 19, 20]. However, TEM microscopy studies have to be performed to confirm this hypothesis.

**Table 2** Transition temperature and enthalpy values of DPPC liposomes with and without PS

Mol %	T <sub>max</sub> (°C)	Linear Onset (°C)	Enthalpy (J/M)
PS			
0	34.4 ± 0.3 pre	33.5 ± 0.6 pre	30 ± 1 pre
0	41.4 ± 0.1 main	40.1 ± 0.1 main	30600 ± 430 main
2,5	41.7 ± 0.1	39.8 ± 0.0	44000 ± 2000
5	41.8 ± 0.0	40.3 ± 0.3	40000 ± 15000
10	42.4 ± 0.1	40.0 ± 0.2	88000 ± 16000
Values are means ± SD n=3, pre=pre transition temp.; main=main transition temp.			

**Table 3** The effect of incorporation of PS into 2.5% (w/w) DPPC liposomes on mean particle size, polydispersity index (PDI) and pH-values

Mol% PS	Particle size (d.nm)	PDI	pH
0	81 ± 6	0.24-0.25	6.3 ± 0.2
2.5	152 ± 7	0.29-0.41	8.4 ± 0.0
5	166 ± 10	0.26-0.48	8.3 ± 0.1
10	178 ± 7	0.34-0.50	8.6 ± 0.0
Values are means ± SD n=5			

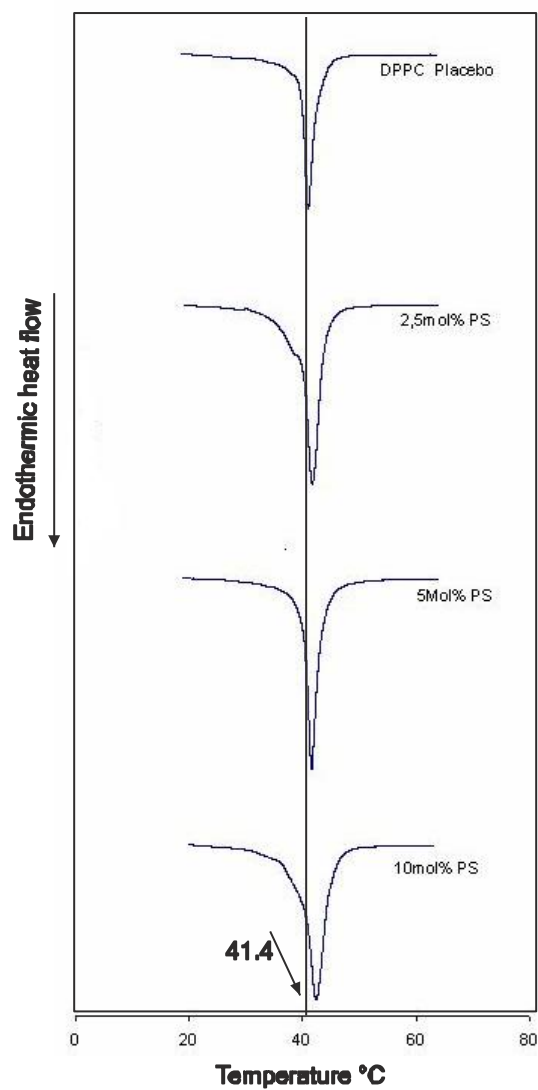


**Figure 2** Representative microDSC endotherms of DPPC liposomes containing 0-10 mol% PS respectively.  $T_{\max}$  of DPPC is 41.4°C as indicated with an arrow

#### **4 Conclusion**

In penetration studies with PS loaded DPPC liposomes it could be proven, that PS is retained in skin in relevant amounts. This seemed to be due to PS-lipid interactions seen in microDSC studies, indicating a closer packing of DPPC and PS in model membranes.

## References

1. Auner B.G. *et al.* Interaction of phloretin and 6-ketocholestanol with DPPC-liposomes as phospholipid model membranes. *Int J Pharm* 2005; 294: 149-155.
2. Biruss B., Valenta C. Comparative characterisation of the physicochemical behavior and skin permeation of extruded DPPC liposomes by selected additives. *J Pharm Sci* 2007; 96: 2171-2176.
3. Cho S. *et al.* Phosphatidylserine prevents UV-induced decrease of type I procollagen and increase of MMP-1 in dermal fibroblasts and human skin in vivo. *J Lipid Res* 2008; 49: 1235-1245.
4. El Maghraby G.M. *et al.* Mechanisms of action of novel skin penetration enhancers: phospholipid versus skin lipid liposomes. *Int J Pharm* 2005; 305: 90-104.
5. El Maghraby G.M. *et al.* Liposomes and skin: From drug delivery to model membranes. *Eur J Pharm Sci* 2008; 34: 203-222.
6. Hoeller S. *et al.* Skin-compatible lecithin drug delivery systems for fluconazole: effect of phosphatidylethanolamine and oleic acid on skin permeation. *J Pharm Pharmacol* 2008; 60: 587-591.
7. Hoeller S. *et al.* Lecithin based nanoemulsions: A comparative study of the influence of non-ionic surfactants and the cationic phytosphingosine on physicochemical behaviour and skin permeation. *Int J Pharm* 2009; 370:181-186.
8. Kang B.Y. *et al.* External preparation containing phytosphingosine as active component for skin. Application: KR (Amorepacific Corp., S. Korea) 2007; 21.
9. Krivanek R. *et al.* Effect of cholesterol and ergosterol on the compressibility and volume fluctuations of phospholipid-sterol bilayers in the critical point region: a molecular acoustic and calorimetric study. *Biophys J* 2008; 94: 3538-3548.
10. Laye C. *et al.* Formation of biopolymer-coated liposomes by electrostatic deposition of chitosan. *J Food Sci* 2008; 73: N7-15.
11. Lucio M. *et al.* Binding of nonsteroidal anti-inflammatory drugs to DPPC: Structure and Thermodynamic Aspects. *Langmuir* 2008; 24: 4132-4139.

12. Min J.K. *et al.* Simultaneous quantitative analysis of sphingoid base 1-phosphates in biological samples by o-phthalaldehyde precolumn derivatization after dephosphorylation with alkaline phosphatase. *Anal Biochem* 2002; 303: 167-175.
13. Panicker L. Interaction of propyl paraben with dipalmitoyl phosphatidylcholine bilayer: A differential scanning calorimetry and nuclear resonance study. *Colloids Surf B* 2008; 61: 145-152.
14. Perugini P.G.I. *et al.* Study on glycolic acid delivery by liposomes and microspheres. *Int J Pharm* 2000; 196: 51-56.
15. Sakaia K. *et al.* Characterizing the structural transition of cationic DPPC liposomes from the approach of TEM, SAXS and AFM measurements. *Colloids Surf B* 2008; 67: 73-78.
16. Schiemann Y. *et al.* Polar emollients in cosmetic formulations enhance the penetration and biological effects of phytosphingosine on skin. *Colloids Surf A* 2008; 2: 103-107.
17. Thompson A.K. *et al.* Comparison of the structure and properties of liposomes prepared from milk fat globule membrane and soy phospholipid. *J Agric Food Chem* 2006; 54: 3704-3711.
18. Wolka A.M. *et al.* The interaction of the penetration enhancer DDAIP with a phospholipid model membrane. *Int J Pharm* 2004; 271: 5-10.
19. Yilmaz E., Borchert H.H. Design of a phytosphingosine-containing, positively-charged nanoemulsion as a colloidal carrier system for dermal application of ceramides. *Eur J Pharm Biopharm* 2005; 60: 91-98.
20. Yilmaz E., Borchert H.H. Effect of lipid-containing, positively charged nanoemulsions on skin hydration, elasticity and erythema-An in vivo study. *Int J Pharm* 2006; 307: 232-238.
21. Yokoyama S. *et al.* Stearylamine Changes the liposomal shape from MLV's to LUV's. *J Oleo Sci* 2005; 54: 251-254.



## 5 Conclusion

The present thesis is concerned with skin application of nanoparticulated systems based on CS-TPP and DPPC, their manufacture and characterisation. In the first part, LC-MS data are used to show that CS-TPP nano-carriers had an improving effect on the chemical properties of aciclovir, slowing its photo-oxidation into the degradation product 9-((2-hydroxyacetyl) methyl)-guanine under day-light exposure in comparison to its aqueous solution. Comparing aciclovir penetration studies in vitro from the CS-TPP nanoparticles demonstrated that nanoparticles with a larger size (~ 650 nm) showed greater aciclovir diffusion through porcine skin than nanoparticles with a smaller size (~ 350 nm). In conclusion the higher CS content as well as a surface charge density of the larger nanoparticles might be the reason of this improved penetration.

Coating of DPPC liposomes with CS and EU improved the liposomes' stability in terms of particle size and PDI. Coated DPPC liposomes with a size of ~ 90 nm showed approximately the same order of aciclovir penetration as the smaller CS-TPP nanoparticles (comparing 10h with 8h studies). The permeation of aciclovir and minoxidil from uncoated DPPC liposomes was significantly lower in comparison with coated DPPC liposomes, what again is inducing on CS ability as the penetration enhancer. Tape-stripping studies on pig ears confirmed these results. Using different formulations the amount of aciclovir in the first layer of the stratum corneum, presented by the first strip, was compared. This demonstrated the following results: CS-DPPC liposomes > DPPC liposomes > aqueous CS-solution. Moreover, conformational changes of skin lipids measured by FTIR spectrophotometer correlated to the penetration depth of aciclovir from the liposomal formulations.

Interaction of drugs as aciclovir, minoxidil and PS, having different logP, with DPPC bilayer was shown by microDSC thermograms. It was first thought that hydrophilic drugs connect with aqueous core whereas strong lipophilic drugs as PS integrate with lipidic domain. The microDSC results displayed either shifting or disappearance of the pre-transition peak as well as alteration of the

main transition peak by all three tested drugs, which could be interpreted as a drug interaction with both regions. If transferred on the skin bilayer we might say that drugs penetrate bonding across lipids, but also with hydrophilic region around corneocytes.

## 6 References

1. Schneider M. *et al.* Nanoparticles and their interactions with dermal barrier. *Dermatoendocrinol* 2009; 4: 197-206.
2. Hoeller S. *et al.* Lecithin based nanoemulsions: A comparative study of the influence of non-ionic surfactants and the cationic phytosphingosine on physicochemical behaviour and skin permeation. *Int J Pharm* 2009; 370: 181-186.
3. Roberts M., Walters K. Dermal absorption and toxicity assessment in: Swabrick J. *Drugs and the pharmaceutical sciences*, Marcel Dekker, Inc. New York. 1998: 1-12
4. Bouwstra J.A. *et al.* Structure of the skin barrier and its modulation by vesicular formulations. *Prog Lipid Res* 2003; 4: 21-36.
5. Meyer R.R. Delivery system handbook for personal care and cosmetic products in: Meyer R.R. *Technology, applications and formulations*, William Andrew, Inc., Norwich, New York. 2005: 78-85
6. Arora A. *et al.* Multicomponent chemical enhancer formulations for transdermal drug delivery: More is not always better. *J Control Rel* 2010; 144: 175-180.
7. Elias P.M. Epidermal Lipids, Barrier Function and Desquamation. *J Invest Dermatol* 1983; 80:44s-49s
8. Laugel C. *et al.* ATR-FTIR spectroscopy: a chemometric approach for studying the lipid organisation of the stratum corneum. *Chem Phys Lipids* 2005; 135: 55-68.
9. Boncheva M. *et al.* Molecular organization of the lipid matrix in intact stratum corneum using ATR-FTIR spectroscopy. *Biochim Biophys Acta* 2008; 1778: 1344-1355.
10. Forslind B. *et al.* A novel approach to the understanding of human skin barrier function. *J Dermatol Sci* 1997; 14: 115-125.
11. Souza S.L. *et al.* Phase Behavior of Aqueous Dispersions of Mixtures of N-Palmitoyl Ceramide and Cholesterol: A Lipid System with Ceramide-Cholesterol Crystalline Lamellar Phases. *J Phys Chem B* 2008; 113: 1367-1375.
12. Wertz P.W. Stratum corneum lipids and water. *Exogenous Dermatol*

- 2004; 3: 53-56.
13. Gardiel P. The thermotropic phase behaviour of phyto-ceramide 1 as investigated by ATR-FTIR and DSC. *Phys Chem Chem Phys* 2002; 4: 2714-2720.
  14. Brandner J. M. Pores in the epidermis: aquaporins and tight junctions. *Int J Cosmet Sci* 2007; 29: 413-422
  15. Kazumasa M., Yoshiki M. Tight junctions in the skin. *J Dermatol Sci* 2003; 31: 81-89.
  16. Kirschner N. *et al.* Tight junctions: is there a role in dermatology? *Arch Dermatol Res* 2010; 302: 483-493.
  17. Brandner J.M. *et al.* A (leaky?) barrier: Tight junction proteins in skin diseases. *Drug discovery today: Disease Mechanisms* 2008; 5: 39-45.
  18. Neubert H.H., Wepf R. Struktur und Morphologie einer Barriere, <http://www.pharmazeutische-zeitung.de/index.php?id=2957&type=0>
  19. Michels C. *et al.* Cadherin-Mediated Regulation of Tight Junctions in Stratifying Epithelia. *Ann New York Academy Sci* 2009; 1165: 163-168.
  20. Niessen C.M. Tight Junctions/Adherens Junctions: Basic Structure and Function. *J Invest Dermatol* 2007; 127: 2525-2532.
  21. Brannon H. //dermatology.about.com/cs/skinanatomy/a/anatomy.htm, 2007
  22. Simon G.A., Maibach H. I. The pig as an experimental animal model of percutaneous permeation in man: qualitative and quantitative observations - an overview. *Skin Pharmacol Appl Skin Physiol* 2000; 13: 229-234.
  23. Jacobi U. *et al.* Porcine ear skin: an in vitro model for human skin. *Skin Res Technol* 2007; 13: 19-24.
  24. Patzelt A. *et al.* Differential stripping demonstrates a significant reduction of the hair follicle reservoir in vitro compared to in vivo. *Eur J Pharm Biopharm* 2008; 70: 234-238.
  25. El Maghraby G.M. Liposomes and skin: from drug delivery to model membranes. *Eur J Pharm Sci* 2008; 34: 203-222.
  26. Lademann J. *et al.* Comparison of two in vitro models for the analysis of follicular penetration and its prevention by barrier emulsions. *Eur J*

- Pharm Sci* 2009; 72: 600-604.
27. Barry B.W. Novel mechanisms and devices to enable successful transdermal drug delivery. *Eur J Pharm Sci* 2001; 14: 101-114.
  28. Benson H.A.E. Transdermal Drug Delivery: Penetration Enhancement Techniques. *Curr Drug Del* 2005; 2: 23-33.
  29. Lademann J. *et al.* Hair follicles - a long-term reservoir for drug delivery. *Skin Pharmacol Physiol* 2006; 19: 232-236.
  30. Lademann J. *et al.* Nanoparticles – An efficient carrier for drug delivery into the hair follicles. *Eur J Pharm Biopharm* 2007; 66: 159-164.
  31. Baroli B. *et al.* Penetration of metallic nanoparticles in human full-thickness skin. *J Invest Dermatol* 2007; 127: 1701-1712.
  32. Ghafourian T. *et al.* Modelling the effect of mixture components on permeation through skin *Int J Pharm* 2010; 398: 28-32.
  33. Cevc G., Vierl U. Nanotechnology and the transdermal route A state of the art review and critical appraisal. *J Cont Rel* 2010; 141: 277-299.
  34. Junginger H.E., Verhoef J.C. Macromolecules as safe penetration enhancers for hydrophilic drugs—a fiction? *Pharm Sci Technol* 1998; 1: 370-376.
  35. Hadgraft J. Skin, the final frontier. *Int J Pharm* 2001; 224: 1-18.
  36. Dhamecha D.L. *et al.* Drug vehicle based approaches of penetration enhancement. *Int J Pharm Pharm Sci* 2009; 1: 24-46.
  37. Moser K. *et al.* Passive skin penetration enhancement and its quantification in vitro. *Eur J Pharm Biopharm* 2001; 52: 103-112.
  38. Barry B.W. Is transdermal drug delivery research still important today? *Drug Discov Today* 2001; 6: 967-971.
  39. Mueller R.H. *et al.* Cytotoxicity of solid lipid nanoparticles as a function of the lipid matrix and the surfactant. *Pharm Res* 1997; 14: 458-462.
  40. Souto E.B. *et al.* Lipid Nanoparticles (SLN®, NLC®) for Cutaneous Drug Delivery: Structure, Protection and Skin Effects. *J Biomed Nanotechn* 2007; 3: 317-331.
  41. Thassu D., Deleers M., Pathak Y. Nanoparticulate drug delivery systems in: Swabrick J. *Drugs and the pharmaceutical sciences* Informa Healthcare USA, Inc., New York, 2007.

42. Alvarez-Roman R. *et al.* Skin penetration and distribution of polymeric nanoparticles. *J Cont Rel* 2004; 99: 53-62.
43. Sonavane G. *et al.* In vitro permeation of gold nanoparticles through rat skin and rat intestine: Effect of particle size. *Coll Surf B: Biointerface* 2008; 65: 1-10.
44. Lademann J. *et al.* Penetration of titanium dioxide microparticles in a sunscreen formulation into the horny layer and the follicular orifice. *Skin Pharmacol Appl Skin Physiol* 1999; 12: 247-256.
45. Gamer A.O. *et al.* The in vitro absorption of microfine zinc oxide and titanium dioxide through porcine skin. *Toxicol in vitro* 2006; 20: 301-307.
46. Hans M.L., Lowman A.M. Biodegradable nanoparticles for drug delivery and targeting. *Curr Opin Sol State Mater Sci* 2002; 6: 319-327.
47. Wu X. *et al.* Disposition of nanoparticles and an associated lipophilic permeant following topical application to the skin. *Mol pharm* 2009; 6: 1441-1448
48. Lopez-Leon T. *et al.* Physiochemical characterisation of chitosan nanoparticles: electrokinetic and stability behavior. *J Coll Intf Sci* 2004; 283: 344-351.
49. Agnihotri S.A. *et al.* Recent advance on chitosan-based micro- and nanoparticles in drug delivery. *J Contr Rel* 2004; 100: 5-28.
50. Enríquez de Salamanca A. *et al.* Chitosan Nanoparticles as a potential drug delivery system for the ocular surface: Toxicity, uptake mechanism and in vivo tolerance. *Invest Ophthalmol Vis Sci* 2006; 47: 1416-1425.
51. Fernandez-Urrusuno R. *et al.* Enhancement of nasal absorption of insulin using chitosan nanoparticles. *Pharm Res* 1999; 16: 1576-1581.
52. Ozbas-Turan S. *et al.* Topical application of antisense oligonucleotide-loaded chitosan nanoparticles to rats. *Oligonucleotides* 2010; 20: 147-153.
53. Luessen H.L. *et al.* Mucoadhesive polymers in peroral peptide drug delivery. VI. Carbomer and chitosan improve the intestinal absorption of the peptide drug Buserelin in vivo. *Pharm Res* 1996; 13: 1668-1672.
54. Sonvico F. *et al.* Formation of self-organised nanopartilces by lecithin/chitosan ionic interactions. *Int J Pharm* 2006; 324: 67-73.

55. Laye C. *et al.* Formation of biopolymer-coated liposomes by electrostatic deposition of chitosan. *J Food Sci* 2008; 73: 7-15.
56. Biruss B. *et al.* Skin permeation of different steroid hormones from polymeric coated liposomal formulations. *Eur J Pharm Biopharm* 2006; 62: 210-219.
57. Hoeller S. *et al.* Skin compatible lecithin drug delivery systems for fluconazole: effect of phosphatidylethanolamine and oleic acid on skin permeation. *J Pharm Pharmacol* 2008; 60: 587-591.
58. Yokomizo Y., Sagitani H. The effects of phospholipids on the percutaneous penetration of indomethacin through the dorsal skin of guinea pig in vitro. 2. The effects of the hydrophobic group in phospholipids and a comparison with general enhancers. *J Cont Rel* 1996; 42: 37-46.
59. Khan D.R. *et al.* Effects of drug hydrophobicity on liposomal stability. *Chem Biol Drug Des* 2008; 71: 3-7.
60. Thomson A.K. *et al.* Comparison of the Structure and Properties of Liposomes Prepared from Milk Fat Globule Membrane and Soy Phospholipids. *J Agric Food Chem* 2006; 54: 3704-3711.
61. Budai M. *et al.* Molecular interactions between DPPC and morphine derivatives: a DSC and EPR study. *Int J Pharm* 2002; 250: 239-250.
62. Meure L.A. *et al.* Conventional and Dense Gas Techniques for the Production of Liposomes: A Review. *Pharm Sci Technol* 2008; 9: 798-808.
63. Souza de E.F., Teschke O. Liposome stability verification by atomic force microscopy. *Rev Adv Mater Sci* 2003; 5: 34-40.
64. Crommelin D.J.A, Zuidam N.J. Hydrolysis of phospholipids in liposomes and stability-indicating analytical techniques in: Gregoriadis G. Liposome technology, Informa Healthcare Inc. New York 2007; 1: 285-295.
65. Abraham W. *et al.* Fusion patterns of liposomes formed from stratum corneum lipids. *J Invest Dermatol* 1988; 90: 259-262.
66. Lopez O. *et al.* Different stratum corneum lipid liposomes as models to evaluate the effect of the sodium dodecyl sulfate. *Biochim Biophys Acta* 2000; 1508: 196-209.

67. Neugebauer D. Externa auf Liposomenbasis haben viele Vorteile, *Deutsche Apotheker Zeitung* 134 1994 973.
68. Verma D.D. *et al.* Particle size of liposomes influences dermal delivery of substances into skin. *Int J Pharm* 2003; 258: 141-151.
69. Egbaria K. *et al.* Topical application of liposomally entrapped cyclosporin evaluated by in vitro diffusion studies with human skin. *Skin Pharmacol* 1991; 4: 21-28.
70. Van den Bergh B.A.I. *et al.* Interaction between liposomes and human stratum corneum studied by freeze-substitution electron microscopy. *Int J Pharm* 1998; 167: 57-67.
71. Korting H.C., Schaller M. Interaction of liposomes with human skin: the role of the stratum corneum. *Adv Drug Delivery Rev* 1996; 18: 303-309.
72. Bhatia A. Tamoxifen in topical liposomes: development, characterisation and in-vitro evaluation. *J Pharm Pharmaceut Sci* 2004; 7: 252-259.
73. Balsari A. *et al.* Protection against doxorubicin-induced alopecia in rats by liposome-entrapped monoclonal antibodies. *Faseb J* 1994; 8: 226-230.
74. Blume A. *et al.* Interaction of phospholipid liposomes with lipid model mixtures for stratum corneum lipids. *Int J Pharm* 1993; 99: 219-228.
75. Niemiec S. *et al.* Influence of nonionic liposomal composition on topical delivery of peptide drugs into pilosebaceous units: an in vivo study using the hamster ear model. *Pharm Res* 1995; 12: 1184-1188.
76. Allen T.M. Liposomal drug formulations: rationale for development and what we can expect for the future. *Drugs* 1998; 55: 747-756.
77. Ioele G. *et al.* Accelerate photostability study of tretinoin and isotretinoin in liposome formulations. *Int J Pharm* 2005; 293: 251-260.



## **7 List of scientific publications, within the present work**

### **7.1 Publications**

- A. Hasanovic, M. Zehl, G. Reznicek, C. Valenta, Chitosan-TPP nanoparticles as possible skin drug delivery system for aciclovir with enhanced stability, J. Pharm. Pharmacol. 2009, 61, 1609-1616
- A. Hasanovic, S. Höller, C. Valenta, Analysis of skin penetration of phytosphingosine by fluorescence detection and influence of the thermotropic behaviour of DPPC liposomes, Int. J. Pharm. 2010, 383, 14-17
- A. Hasanovic, C. Hollick, K. Fischinger, C. Valenta, Improvement of physicochemical parameters of DPPC liposomes and increase of skin permeation aciclovir and minoxidil by addition of cationic polymers, Eur. J. Pharm. Biopharm. 2010, 75, 148-153
- A. Hasanovic, R. Winkler, G. Resch, C. Valenta, Modification of the conformational skin structure by treatment with liposomal formulation and its correlation to the penetration depth of aciclovir, submitted for publication

### **7.2 Poster presentations**

- Chitosan-TPP nanoparticles as possible skin drug delivery system for aciclovir with enhanced stability (Skin and Formulation 3<sup>rd</sup> Symposium and Skin Forum, 10<sup>th</sup> Annual Meeting, Versailles 2009)
- Polymer coated DPPC liposomes as the skin delivery formulation for aciclovir and minoxidil (Skin Forum, 11<sup>th</sup> Annual Meeting, Edinburgh 2010)

### **7.3 Oral presentations**

- Increased skin permeation of aciclovir through incorporation into chitosan-tripolyphosphate nanoparticles (Austrian Pharmaceutical Society, 21<sup>th</sup> Annual Meeting, Vienna 2009)

## **8 List of Scientific publications, beyond the present work**

### **8.1 Publications**

- H. Kählig, A. Hasanovic, B. Biruss, S. Höller, J. Grim, C. Valenta, Chitosan-glycolic acid: a possible matrix for progesterone delivery into skin, Drug. Dev. Ind. Pharm. 2009, 1, 1-6

### **8.2 Poster presentations**

- Chitosan glycolic acid as possible matrix for progesterone and 17 $\beta$ -estradiol (6<sup>th</sup> world meeting on Pharmaceutics, Biopharmaceutics and Pharmaceutical Technology, Barcelona 2008)

## 9 Abbreviations

---

ATR	Attenuated total reflectance
CS	Chitosan
CS-TPP	Chitosan-Tripolyphosphate
DPPC	Dipalmitoylphosphatidylcholine
DSC	Differential scanning calorimetry
EE	Encapsulation efficiency
EU	Eudragit EPO
FTIR	Fourier transform infrared spectrometry
LC	Loading capacity
LC-MS	Liquid chromatography-mass spectrometry
MPS	Mean particles size
OPA	o-phthalaldehyde
PS	Phytosphingosine
PDI	Polydispersity Index
SC	Stratum corneum
TPP	Tripolyphosphate
ZP	Zeta potential

---

## CURRICULUM VITAE

**Amra Hasanovic**

### Personal Data

- Date of birth: 07. 03.1980, Tuzla, Bosnia and Herzegovina
- Nationality: Bosnian

### Education

- Since 03/2007: PhD-Thesis, Department of Pharmaceutical Technology and Biopharmaceutics, University of Vienna, Austria
- 03/2006 - 03/2007: Aspirant educations, in `Apotheke zum St. Nikolaus`, Pottendorf, Austria
- 08/2005: Master degree, University of Vienna, Austria
- 2005: Diploma Thesis, Department of Pharmacology and Toxicology, University of Vienna, Austria
- 10/2000–08/2005: Academic studies (Pharmacy), University of Vienna, Austria
- 10/1998 – 03/2000: Academic studies (Pharmacy), University of Sarajevo, Bosnia and Herzegovina
- 1994-1998: Secondary school (Tuzla, Bosnia and Herzegovina)

## Professional Experience

- Since 09/2009      Lecturer for `Workshop in Pharmaceutical Technology for Dermatologists` Department of Pharmaceutical Technology and Biopharmaceutics, University of Vienna, Austria
- Since 09/2007      Lector for the practical course on `Magistral formulae`, Department of Pharmaceutical Technology and Biopharmaceutics, University of Vienna, Austria
- Since 03/2007      Part time job as Pharmacist in `Apotheke zum St. Nikolaus`, Pottendorf, Austria